# Mass balances of Yala and Rikha Samba Glacier, Nepal from 2000 to 2017

Dorothea Stumm[1,2], Sharad Prasad Joshi[2], Tika Ram Gurung[2], Gunjan Silwal[2,3]

[1]Independent consultant, 8184 Bachenbülach, Switzerland
[2]ICIMOD, G.P.O. Box 3226, Kathmandu, 44600, Nepal
[3]Department of Earth and Atmospheric Sciences, University of Alberta, Edmonton, Alberta, T6G 2E3, Canada

*Correspondence to*: Dorothea Stumm (stummd@gmail.com)

**Abstract.** The direct or glaciological method is an integral part of international glacier monitoring strategies, and the mass balance is an essential variable to describe the climate system and model runoff. In 2011, we established two glacier mass balance programmes on Yala and Rikha Samba Glacier in the Nepal Himalaya. Here we present the methods and data that we ingested into the database of the World Glacier Monitoring Service. We present glacier length changes and the annual mass balances for the first six mass balance years for both glaciers. For Yala Glacier we additionally present the mass balance of seasonal in situ measurements and the mass balance from 2000 to 2012 analysed with the geodetic method. The annual mass balance rates of Yala Glacier from 2000 to 2012 and from 2011 to 2017 are -0.74 ±0.53 m and -0.74 ±0.28 m w.e. a$^{-1}$, and for Rikha Samba Glacier from 2011 to 2017 -0.39 ±0.32 m w.e. a$^{-1}$. The mass loss for the period 2011 to 2017 for Yala and Rikha Samba Glacier -4.44 ±0.69 m w.e. and -2.34 ±0.79 m w.e., respectively. The winter balance of Yala Glacier is positive in every investigated year, but the negative summer balance determines the annual balance. The mass balance of Yala Glacier is more negative than on other glaciers in the region, mostly because of the small and low lying accumulation area. The mass balance of Rikha Samba Glacier is more positive than the other glaciers in the region, likely because of the large and high lying accumulation area. Due to the topography, the retreat rates of Rikha Samba Glacier are much higher than for Yala Glacier. From 1989 to 2013, Rikha Samba retreated 431 m (-18.0 m a$^{-1}$), and from 1974 to 2016 Yala Glacier retreated 346 m (-8.2 m a$^{-1}$). During the study period, a change of Yala Glacier's surface topography has been observed with glacier thinning and downwasting, which indicates the likely disappearance of Yala Glacier within this century. The datasets are freely accessible from WGMS (2020a): Fluctuations of Glaciers Database. World Glacier Monitoring Service, Zurich, Switzerland. http://dx.doi.org/10.5904/wgms-fog-2020-08.

## 1 Introduction

Glaciers are an essential climate variable (ECV) that contribute to understand and describe the global climate system (IGOS, 2007; GCOS, 2016). The glaciological method for glacier mass balance monitoring is an integral part of international glacier monitoring strategies and a significant component to estimate global sea level rise, regional river runoff and local hazards. As an important variable the mass balance is used to model the water availability and runoff scenarios for glacierized catchments and downstream livelihoods and ecosystems (Huss and Hock, 2018; Immerzeel et al., 2012; Kaser et al. 2010). The World Glacier Monitoring Service (WGMS) manages the data warehouse for glacier monitoring data including mass balance and frontal variation data, and runs the Global Terrestrial Network for Glaciers (GTN-G) in collaboration with partners. GTN-G is the framework for the internationally coordinated monitoring of the ECV glacier, and supports the United Nations Framework Convention on Climate Change (UNFCCC).

The current contribution of glaciers in the Hindu Kush Himalayan (HKH) region to the water availability downstream and sea level rise involve still large uncertainties (Zemp et al., 2020; Immerzeel et al., 2019; Azam et al., 2018; Marzeion et al., 2012; Bolch et al., 2012). Still only few long-term programmes are established to monitor the in situ glacier mass balance and length changes on clean glaciers in Bhutan, China, India, Nepal and Pakistan (e.g. Azam et al., 2018; Wagnon et al., 2020; Tshering

40 and Fujita, 2016; Dobhal et al., 2013), and only few include seasonal measurements (Wagnon et al., 2013; Azam et al., 2016; Sherpa et al., 2017). On a regional scale glacier mass balances have been estimated by remote sensing techniques (e.g. Abdullah et al., 2020; Maurer et al., 2019; Gardelle et al., 2013; Vincent et al., 2013; Kääb et al., 2012; Berthier et al., 2007) and modelling (Fujita et al., 2011; Shea et al., 2015a; Tawde et al., 2017). However, due to the remoteness, high altitude topography and logistical challenges there is still a lack of in situ measurements to validate and calibrate such studies. Some studies focus

45 on ablation and runoff on a high spatial and temporal resolution, especially on debris covered glaciers (Litt et al., 2019; Pratap et al., 2019; Pratap et al., 2015; Immerzeel et al., 2014; Fujita and Sakai, 2014; Lutz et al., 2014), but rarely measure precipitation and snow accumulation in high altitudes due to challenges such as harsh conditions for precipitation measurements or difficult access to the accumulation zone.

A detailed review on the status and mass changes of Himalayan glaciers has been provided by Azam et al. (2018). They found

50 that up to the year 2000, the mean glacier mass balance was in a similar range as the global average, but likely less negative after 2000. The longest time series with direct glaciological measurements are found for Chhota Shigri Glacier, India, since 2002 (Wagnon et al., 2007; Azam et al., 2012, 2014 and 2016). Other investigated glaciers in the Indian Himalaya partly with ongoing monitoring are for example Dokriani, Gara, Gor Garang, Naradu, Neh Nar, Shaune Garang and Tipra Bank (Dobhal et al., 2008; Vincent et al., 2013; Pratap et al., 2015; Azam et al. 2018; WGMS, 2020a). In the Chinese Himalaya, glaciological

55 and dGPS mass balance records are available from 1991 to 1993 and 2007 to 2010 for Kangwure Glacier, north of Mt Shisha Pangma and Langtang Valley, and from 2006 to 2010 on Naimona 'Nyi Glacier, in an upper tributary of the Ganges (Liu et al. 1996; Tian et al., 2014; WGMS, 2020a). Glaciological and in situ geodetic mass balance measurements have been carried out in Bhutan on Gangju La Glacier from 2003-2014 (Tshering and Fujita, 2016) and Thana Glacier since 2012 by the National Center for Hydrology and Meteorology by the Government of Bhutan, and the partners ICIMOD and the Norwegian Water

60 Resources and Energy Directorate. In Afghanistan, index measurements were initiated in 2017 on Pir Yakh Glacier and are continued by the University of Kabul, the Ministry of Energy and Water and supported by ICIMOD (WGMS, 2020b).

In the Nepal Himalaya extensive glaciological measurements have been carried out by Japanese researchers on Rikha Samba Glacier, Hidden Valley and AX010 in Shorong Himal since the 1970's, and on Yala Glacier, Langtang Valley since the 1980's (e.g. Ageta and Higuchi, 1984; Fujii et al., 1996; Fujita et al., 1998; Fujita et al., 2001; Sugiyama et al., 2013). Mass balance

65 programmes were established on Mera Glacier in Hinku Valley, Pokalde and West Changri Nup Glacier in Khumbu Valley in 2007, 2009 and 2010, respectively (Wagnon et al., 2013; Sherpa et al., 2017). Wagnon et al. (2020) use a comprehensive monitoring approach for Mera Glacier by reanalysing the mass balance data and calibrating the glaciological measurements from 2007 to 2019. Various researchers used the geodetic method with remote sensing products or in situ surface surveys to calculate thickness changes (e.g. Bolch et al., 2008; Bolch et al., 2011; Nuimura et al., 2012; Lindenmann, 2012; Ragettli et

70 al., 2016).

On Rikha Samba Glacier, the first glaciological fieldwork was carried out in 1974 by Japanese researchers as part of the Glaciological Expedition of Nepal (GEN) (Fujii et al., 1976). Further fieldwork was carried out in October 1995, including terminus surveys, glacier surface profiles, flow measurements, ice core drilling and meteorological observations (Fujii et al., 1996; Fujita et al., 1997a; Shrestha et al., 1976). In October 1998 and 1999, stakes were installed and measured for direct point

75 mass balance measurements (Fujita et al., 2001). Terminus position changes and surface flow velocities were also measured and weather data collected. In 2010, the glacier surface was again surveyed with dGPS and the geodetic mass balances calculated (Fujita and Nuimura, 2011) and meteorological data collected.

Yala Glacier was selected based on a GEN reconnaissance flight in Langtang Valley because it was the only one without debris cover and it had easy access to the accumulation area (Watanabe et al., 1984). Comprehensive studies were carried out with a

80 wide range of measurements, for example glacier processes, meteorology, geomorphology and photogrammetry (e.g. Murakami et al., 1989; Ono, 1985; Yokohama, 1984). Stake measurements were taken in September and October 1982 (Ageta et al., 1984), and from summer 1985 to spring 1986 (Iida et al., 1987). In the accumulation area, Okawa (1991), Iida et al.,

(1984), Watanabe et al. (1984), and Steinegger et al. (1993) investigated the snow cover, boreholes, crevasses and ice cliffs to better understand the processes including mass balance, hydrology and snow metamorphosis. Fujita et al. (1998) carried out

85 further glaciological measurements in 1994 and 1996 and documented an accelerated retreat and surface lowering of Yala Glacier in the 1990s and decreasing flow velocities. Various studies (e.g. Shiraiwa and Watanabe, 1991; Ono, 1985; Yamada et al., 1992; Kappenberger et al., 1993) document historic and recent glacier fluctuations at Yala Glacier and for Langtang Valley. Hydro-meteorological observations were made by Japanese researchers in 1982, 1985 to 1986, 1989 to 1991, and 2008 to 2011 (Yamada et al., 1992; Takahashi et al., 1987a; 1987b; Fujita et al., 1997b; Shiraiwa et al., 1992; unpublished data).

90 Based on sensitivity studies and observational data from Yala and other Himalayan glaciers Fujita (2008a, 2008b) highlights the importance of precipitation seasonality on the climatic sensitivity of glacier mass balance, besides air temperature changes. In the Fourth Assessment Report of the Intergovernmental Panel on Climate Change (Cruz et al., 2007; Cogely et al., 2010), misinformation was published about an extreme above global average shrinkage of Himalayan glaciers. This led to the question about the actual status and future development of the glaciers in the Himalayas. Since then, many studies have been published

95 on the glacier status and changes with remote sensing techniques and modelling approaches. However, in situ monitoring programmes of glacier mass balances and high-altitude weather stations are still rare. The main objective of this study was to establish sustainable and long-term glacier mass balance programmes on Yala and Rikha Samba Glacier and submit the standardized data to the World Glacier Monitoring Service (WGMS, 2015; 2017; 2020a; 2020b). An integral part of the programme was to conduct trainings every year on the easily accessible Yala Glacier for a few dozens of students and

100 professionals from the Himalayan countries, on one hand to build capacity for sustainable and consistent measurements, and on the other hand to promote the development of further mass balance programmes in other parts of the Hindu Kush Himalayan Region. Students from Kathmandu University utilized preliminary mass balance data for their Master theses' (Baral et al., 2014; Gurung et al., 2016; Acharya and Kayastha, 2019).

Here we focus on Yala Glacier where combined bi-annual mass balance field measurements and remote sensing approaches

105 allowed to assess the mass balance of this glacier from 2000 to 2017, and glacier length changes from 1974 onwards. On Rikha Samba Glacier we assess the annual mass balances and glacier length changes from 2011 and 1989 onwards, respectively. The methods are documented for the data submitted to the WGMS (WGMS, 2020a; 2020b). The descriptions of challenges, methods and decisions confronted within a Himalayan context may serve as reference for colleagues starting new glacier monitoring programmes in the Himalayas.

110 **2 Study areas and climatic setting**

Yala Glacier is a small and debris-free glacier in central Nepal in Langtang Valley, and Rikha Samba Glacier is a valley glacier with a moderate altitude range located in western Nepal, in the Hidden Valley in Lower Mustang (Fig. 1, Table 1). Both glaciers are under the influence of the South Indian summer monsoon. However, Rikha Samba Glacier lies behind the main weather divide in the rain shadow zone and receives less precipitation. Yala Glacier has been studied since 1981 (Higuchi et

115 al., 1984), and Rikha Samba Glacier already in 1974 and from 1994 onwards, with long gaps (Fujita et al., 1997a). In 2011, for both glaciers, monitoring programmes were re-started, in the framework of the HKH-Cryosphere Monitoring Project (CMP), by ICIMOD, and its partners the Department of Hydrology and Meteorology of the Government of Nepal, Kathmandu University and Tribhuvan University.
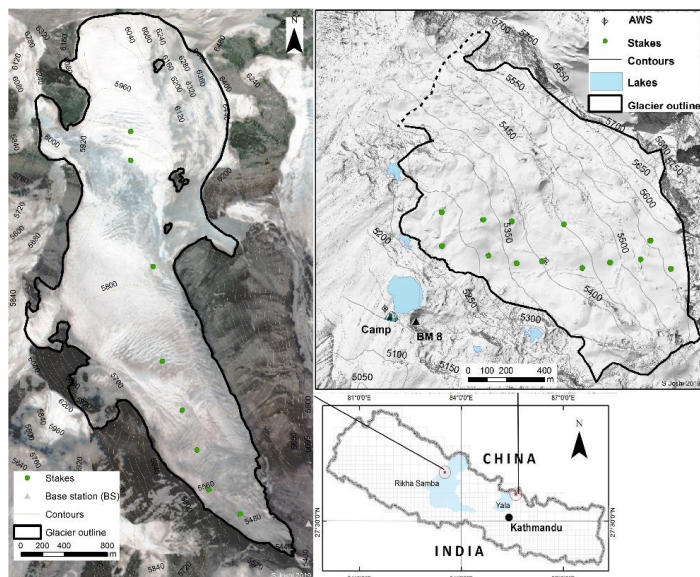
120 **Figure 1: Study sites Rikha Samba (left) and Yala Glacier (right), showing the measurement network and glacier boundaries from 2010 (Rikha Samba) and 2012 (Yala). The background images are the hill-shaded DEM derived from the SRTM-3 and GeoEye-1 image of January 2012 for Rikha Samba and Yala Glacier, respectively.**

Table 1. Geographic and topographic features of Yala Glacier in Langtang Valley and Rikha Samba Glacier in the Hidden Valley.

| General features of | Yala Glacier | Rikha Samba Glacier |
|---|---|---|
| Country, region | Nepal, Rasuwa district | Nepal, Mustang district |
| Mountain range | Langtang Himal, Central Nepal Himalaya | Dhaulagiri, Western Nepal Himalaya |
| River system | Trisuli basin, Ganges river | Kali Gandaki basin, Ganges river |
| Climate | Indian monsoon zone | Rain shadow |
| Glacier type | Summer-accumulation type | Summer-accumulation type |
| Glacier characteristics and mass balance information | | |
| Latitude/ Longitude | 28° 14' N, 85° 34' E | 28° 50' N, 83° 30' E |
| Elevation range | 5168–5661 m a.s.l. | 5416–6515 m a.s.l. |
| Glacier area/length | 1.61 $km^2$/1.4 km (2012, GeoEye) | 5.7 $km^2$/5.4 km (2010, Rapid Eye) |
| Orientation | South west | South east |
| $ELA_0$ | ~5380 m a.s.l. | ~5760 m a.s.l. |
| $AAR_0$ | 49 % | 66 % |
| Measurement information | | |
| Maximum number of measurement sites | 14 (between 5175–5483 m a.s.l.) | 8 (between 5437–5900 m a.s.l.) |
| Measurement frequency | Biannually in May and November (pre- and post-monsoon) | Annually in October (post-monsoon) |

### 2.1 Yala and Rikha Samba Glacier

140    Yala Glacier (28° 14' N, 85° 36' E) is located in the Rasuwa district, Central Nepal about 70 km north of Kathmandu, draining into Langtang River which feeds the Trisuli, and then Ganges River. It is a plateau-shaped glacier, ranging from 5168 m to 5661 m a.s.l, and with a length and area of about 1.4 km and 1.61 $km^2$ respectively. The glacier extends further to north-west, however, for the analyses, the glacier has been separated along the flowline, based on the surface contour line method. The slopes of the glacier face mainly southwest, and have numerous ice cliffs and slopes steeper than 50° that make up 5 % of the

145    glacier area, whereas the vertical cliffs cannot be quantified in the DEM. The mean and maximum ice thickness was 36 m and

61 m in 2009 and the glacier bed topography indicates several small overdeepenings (Sugiyama et al., 2013). The glacier is polythermal (Okawa, 1991; Sugiyama et al., 2013), has clean ice with little debris and small proglacial ponds. In the 2015 Nepal earthquake, rockfall covered parts of the glacier, which are outside the defined outlines. In these parts we find a transition from glacier ice with debris cover to possible permafrost with refrozen meltwater and buried ice. Yala Glacier sits on a gneiss
150   bedrock shelf, which forms part of the base from which the earth's largest landslide in a crystalline environment slipped (Weidinger et al., 2002, Takagi et al., 2007). Weidinger et al. (2002) suggest that the landslide was a mountain of about 8000 m height, which collapsed about 51 ±13 Ka ago (Takagi et al., 2007). The dislocated mass lies southwest of Yala Glacier and has largely been eroded in the most recent high glaciation. The landslide left behind an open topography, which together with the southwest aspect of the glacier allows Yala Glacier to receive a lot of solar radiation. The surrounding high mountains of
155   the Langtang range (>6500 m a.s.l.) possibly shelter Yala Glacier from strong high winds and precipitation.

Rikha Samba Glacier (28° 50' N, 83° 30' E) is located in the Hidden Valley on the north side of the main range, and is part of Lower Mustang. The Sangda River drains the Hidden Valley and joins the Kali Gandaki River further down. The glacier is polythermal (Gilbert et al., 2020), ranges from 5416 m to 6515 m a.s.l. and has a length and area of 5.4 km and 5.7 km². At about 6000 m at the head of the valley, the glacier is wide and flows down with a gentle slope of ~10° on average, facing
160   mainly south, and southeast at the glacier tongue. Above 6000 m a.s.l, the glacier is steep with an average slope of ~36° making up 19 % of the glacier area, and flowing down from the sides of the valley. The climate at Rikha Samba and in the Hidden Valley is drier and windier.

## 2.2 Climate

The Himalayan mountains are an orographic barrier causing strong north-south, but also altitudinal temperature and
165   precipitation gradients. Nepal is under the influence of the Indian summer monsoon that brings the majority of the annual precipitation, and receives in winter some precipitation from westerlies (Bookhagen and Burbank, 2010). The inter-annual variability of precipitation is much larger in winter than in summer, caused by westerly disturbances and occasional cyclones originating in the Bay of Bengal (Seko and Takahashi, 1991; Fujita et al., 1997b). However, climate information from high elevations in the HKH are sparse. The few high-altitude climate stations are mostly situated in valley floors and satellite derived
170   products are less reliable (Salerno et al., 2015; Shea et al., 2015b; Ménégoz et al., 2013). Snowfall studies quantifying timing and amounts are sparse but critical (Litt et al., 2019), and automated snowfall measurements are challenging because undercatch can be up to 20 to 50 % in windy conditions (Rasmussen et al., 2012).

Immerzeel et al. (2012) found that the upper Langtang Khola catchment received 814 mm of precipitation per year, and 77 % of it during monsoon from June to September based on ERA40 data from 1957-2002. The climate station nearest to Yala
175   Glacier with long-term data is in Kyangjing at 3,920 m a.s.l., which is about 6 km horizontal distance and south west from Yala Glacier. Racoviteanu et al. (2013) analysed the climate station data at Kyangjing between 1988 and 2006 and found an average annual precipitation of 647 mm. Fujita & Nuimura (2011) estimated the long-term annual precipitation at Yala Glacier to be 772 mm. The conditions at the leeside of the main mountain range at Rikha Samba Glacier are much drier. Precipitation measured with a totalizer and a tipping bucket in the vicinity of the terminus of Rikha Samba Glacier (5267 m a.s.l.) amounted
180   to about 450 mm from October 1998 to September 1999 (Fujita et al., 2001). The precipitation measured from October to April is minimal and likely indicates underrepresented snowfall. Fujita and Nuimura (2011) estimated at least 370 mm of long-term annual precipitation at Rikha Samba Glacier, and Shrestha et al., (1976) measured 203 mm of precipitation at 5055 m a.s.l. in the Hidden Valley during monsoon from July to early September 1974.

The mean annual air temperature in Kyangjing was about 4 °C from 1988 to 2012. Near Rikha Samba Glacier's terminus, the
185   annual mean air temperatures were –4.6° C and –5° C, at 5267 m a.s.l. in 1999 and at 5310 m a.s.l. in 2014, respectively (Fujita et al., 2001; Gilbert et al., 2020). Temperature lapse rates vary with the season, with largest and smallest lapse rates in winter

and summer, respectively (Immerzeel et al., 2015). The diurnal temperature variabilities are smallest during monsoon (Shea et al., 2015b).

Generally, in the Nepal Himalaya the sky is clear in the post-monsoon and winter season, indicated by the incoming solar
190 radiation. Cloudiness increases during pre-monsoon and reaches a maximum during monsoon. During monsoon, the cloudiness at Yala Glacier is much higher than at Rikha Samba Glacier, which can be explained by the valley circulation and cloud formation patterns in Langtang and the leeside location of Rikha Samba Glacier (Fujita et al., 2001; Shea et al., 2015b; Litt et al., 2019). During post-monsoon and winter, the incoming solar radiation is higher at Yala Glacier, which can be explained by the open topography.

195 Throughout the year, the wind velocities at Rikha Samba Glacier are higher and with a larger variability than at Yala Glacier. (Shea et al., 2015b). The highest wind speeds are recorded in winter from October to May, with strong wind events with >8 ms⁻¹ (Fujita et al., 2001). Winter wind velocities measured at Rikha Samba Glacier are very high and possibly caused by strong winds associated to the subtropical jet stream (Ding and Sikka, 2006). The winter wind speeds at Yala Glacier are much smaller, possibly because Yala Glacier is better sheltered by surrounding high mountains. During monsoon from June to
200 September the windspeeds are lower with a smaller variability.

## 3 Data and methods

The mass balance of the two glaciers is monitored from 2011 to 2017 with the direct, glaciological method using stakes, snow pits and cores, and for Yala Glacier also with the geodetic method from 2000 to 2012. The frontal variations were evaluated based on satellite images, GPS and dGPS data.

205 ### 3.1 Data collection

The in situ measurements of the HKH-CMP started in autumn 2011 and are conducted biannually on Yala and annually on Rikha Samba Glacier. On Yala Glacier, the annual/summer balance measurement were taken in November. The winter balance was measured in late April or early May, and in 2015 in early June due to the major earthquake in Nepal on 25 April 2015. On Rikha Samba Glacier, in the first years the measurements were carried out in September, which is rather early because still
210 under the influence of the monsoon. In the following years, the measurements were carried out in October or November. Generally, October and November are ideal periods for mass balance measurements in the central Nepal Himalaya, but coincide with the main festival season in Nepal. The festival season is of great religious importance, lasts for several weeks, and varies every year by weeks. This makes it hard to plan fieldwork at fixed dates and find people to conduct measurements. The autumn expeditions with trainings on Yala Glacier were conducted after the last festival ended to allow training
215 participation from various institutions and universities.

### 3.1.1 In situ mass balance

In the ablation area, the mass balance is measured with bamboo stakes. If snow is present, its depth is usually measured at each measurement site, at selected sakes the snow density and profile are also recorded. In the accumulation area, bamboo stakes mainly mark the measurements sites, but in absence of snow pit data they are also used for the mass balance calculation, in
220 particular in the case of a negative mass balance. The snow pit measurements are only reliable if the previous measurement horizon can clearly be identified, e.g. when marked with a sawdust layer. Difficulties arise in the accumulation area, if ablation and accumulation occur in the same period. If there is ablation before new accumulation, this ablation is not represented in a snow pit measurement and likely impacts the sawdust layer. Stake readings are less reliable because the underlying snow and firn layers compact over time and may push or pull the stake up or down.

On Yala Glacier, the measurement network stretches along a line that has been measured in the past by Japanese Researchers (Fujita et al., 1998). In the lower part a few stakes were added in a transect. Since the glacier has been shrinking, a second row of stakes was installed parallel to the original line in November 2016, in an attempt to maintain measurements also in future when the glacier retreats beyond the current stake locations. Large parts of the glacier are difficult to access because of ice cliffs, crevasses, and steep terrain. There is likely high ablation at the ice cliffs and steep slopes, which creates a bias that cannot be quantified.

On Rikha Samba Glacier, eight stakes are installed along the approximate glacier flowline, which follow roughly the setup of the Japanese researchers (Fujita et al., 2001). In the first year, the lower five stakes were installed, and in 2012 additional 3 measurement sites established. In 2011 and 2014, the conditions on the glacier were very difficult and the higher part of the glacier could not be reached. Snow depth, and snow pits with density were measured, but sawdust was spread only during few occasions and found only once, making accumulation measurements challenging.

At Yala Glacier, the measured average densities with standard deviation for snow and firn were 336 kg m$^{-3}$ (±81 kg m$^{-3}$) and 562 kg m$^{-3}$ (±128 kg m$^{-3}$). However, harder firn layers were difficult to measure and dependent of the site and conditions, firn densities were estimated between 550 kg and 700 kg m$^{-3}$. For ice we assumed a density of 900 kg m$^{-3}$. At Rikha Samba Glacier, the average snow density measured was 399 kg m$^{-3}$ with a standard deviation of ±70 kg m$^{-3}$.

### 3.1.2 GPS surveys

Differential GPS (dGPS) were used to survey the glacier termini, measurement sites, benchmarks, thickness changes along profiles, and surface velocities (Table S1). The devices were dual frequency dGPS, from Topcon and Magellan ProMark 3, and used in real time kinematic (RTK) mode. The instrument accuracy is within a 10 mm range in RTK mode after post-processing. In the field the antenna was kept vertical in the backpack as much as possible and thus the accuracy is estimated to be ±0.3 m at worst. At every visit, the measurement sites were also surveyed with handheld Garmin GPS, occasionally also the glacier terminus. The elevations of the handheld GPS were not used because of the higher uncertainty and inconsistent geoid correction by various users. At Yala Glacier, the number of visible satellites was normally very high, possibly due to the open topography, hence the GPS data often have a relatively high accuracy for a handheld GPS.

Yala Glacier's terminus is very broad and hence the terminus has been mapped covering the lowest part of the glacier, and beyond in an attempt to map part of the glacier outlines. The mapping was done with a Garmin GPS in November 2012 and a Topcon dGPS in May 2014 and 2016. On Rikha Samba Glacier, the terminus was surveyed with a Topcon dGPS in September 2013.

The glacier surface profiles of Yala and Rikha Samba Glacier were repeatedly surveyed with dGPS, along a longitudinal profile and three and two cross-profiles, respectively, but only data from May 2012 from Yala Glacier are presented here. Annual surface velocities were derived from stake displacement between 8 May 2012 and 5 May 2014 on Yala Glacier.

### 3.2 Maps, satellite images and DEMs

For Yala Glacier, various maps have been compared and evaluated for their suitability for area, volume and frontal change analysis. The maps include the Survey of India, Schneider and Nepal topographical maps published in 1965, 1990 and 1995, the map by the Japanese Glaciological Expedition Nepal (GEN) map (Yokoyama, 1984) and glacier outlines from the ICIMOD glacier inventory of Nepal (Bajracharya et al., 2014; Table S2). The GEN map and glacier inventory data were used; however, despite good quality no other maps could be used because of transformation issues and inconsistencies. The GEN map is based on a ground photogrammetric field survey in 1981 and has a scale of 1:5,000 (Yokoyama, 1984). The photo point was about 2 km from the glacier terminus in 1981 on a lower location; consequently, the exposing axis is almost parallel to the glacier surface. We found a distortion and mismatch at the ridge and at the southeast and northwest side of the glacier. To calculate the frontal variations, we georeferenced the map with the GeoEye-1 orthoimage from 2012.

Satellite images were used to delineate glacier outlines, termini, and other tasks for both glaciers, and the geodetic mass balance of Yala Glacier (Table S3). For the glacier-wide geodetic mass balance analysis, stereo satellite images were evaluated with a date overlapping with the fieldwork period either in October/November or April/May, or in early winter when there is little new accumulation and ablation, clear sky conditions, and ideally few shadows.

270 The SRTM-3 DEM (SRTM-3) is the third version of the DEM from the Shuttle Radar Topography Mission (SRTM) and is generated based on data from 2000. The spatial resolution is about 90 m, with an absolute vertical accuracy of ±16 m and a vertical reference to the WGS 84 EGM96 geoid (Rabus et al., 2003). The penetration of the SRTM C-band beam in snow, firn and glacier ice is an issue that results in a lower accuracy especially in the accumulation area (Kääb et al., 2012, Berthier et al., 2006). SRTM-3 was resampled to 30 m for the geodetic mass balance calculation of Yala Glacier. The SRTM-1 DEM was

275 used for the mass balance analysis of Rikha Samba Glacier. It is based on the SRTM-3 data from 2000 but has been released with an improved resolution of about 30 m. Aster images were also evaluated but clouds and fresh snow made the products unsuitable for use.

The GeoEye-1 is a commercial high-resolution stereo satellite image with 0.5 m spatial and 8 bits per pixel radiometry resolutions. The stereoscopic images from 15 January 2012 were used to generate a DEM (DEM2012) for Yala Glacier to

280 calculate the glacier-wide geodetic mass balance. The orthoimage from GeoEye-1 was used in combination with dGPS data to delineate the outlines of Yala Glacier.

We analysed images from several generations of Landsat, which are American Earth observation satellites. Landsat 4 has a resolution of 79 m, and the later Landsat 5 Thematic Mapper (TM) and Landsat 7 Enhanced Thematic Mapper (EMT+) have a resolution of 30 m. The Landsat 8 was made available for the public since 2013. It has eleven bands panchromatic,

285 multispectral and thermal with spatial resolutions of 15 m, 30 m and 100 m respectively and the panchromatic band 8 has 0.500– 0.680 µm radiometric resolution. The visible band of the image acquired on 18 November 2013 has been used to collect horizontal reference (x, y) and the SRTM-3 for the vertical reference (z) for ground control points to georeferenced the GeoEye-1 images, and tie points for DEM generation for Yala Glacier. The ICIMOD glacier inventory for Nepal (Bajracharya et al., 2014) is based on Landsat 7 ETM+ images from 2000, and the outlines of Yala Glacier have been used and modified

290 based on the original data. The outlines have been used for the geodetic mass balance and frontal variation analyses. The inventory outline data from the years 1980, 1990 and 2010 were not used because of the coarse resolution of the base images, partial snow cover and high uncertainty of ±30-60 m. We used a Landsat 4, Landsat 7 ETM+ and two Landsat 5 TM images from the years 1989, 2001, 2006 and 2011 to analyse terminus changes of Rikha Samba Glacier. RapidEye images from 25 and 27 April 2010 were used to delineate the outlines of Rikha Samba Glacier.

295 Hexagon KH-9 images from November 1974 were used for a frontal variation analysis of Yala Glacier but were found unsuitable for area and volume analysis because of void areas, or cloud and snow cover in the images at other times of the year. Additionally, it was difficult to delineate the glacier at the north-west and south-east side without contour lines to derive the flowlines at that time.

For this study, we adopt the projection system WGS 1984, UTM Zone 44N and 45N for Rikha Samba and Yala Glacier,

300 respectively. The projection is the Modified Transverse Mercator, with false easting 500,000 m and scale factor of 0.9999 at the central meridian 84° E and 87° E for Rikha Samba and Yala Glacier, respectively.

### 3.3 DEM generation

The DEM generation from GeoEye-1 stereo images from 2012 involved four steps, following Holzer et al. (2015): collection of ground control points (GCPs), extraction of the DEM, and the two post-processing steps to clean DEM areas of low quality

305 and to co-register the DEM. The DEM was used for the mass balance analysis with the geodetic and glaciological method.

Eight ground control points (GCPs) were used to georeference the GeoEye-1 stereo satellite images. The GCPs were obtained from stable terrain and are evenly distributed. The x and y coordinates of the GCPs were measured from a Landsat 8 image from November 2013, and the z-values were taken from the SRTM-3 DEM. All GCPs were cross-checked in Google Earth™. For the DEM extraction from the GeoEye-1 stereo images OrthoEngine from PCI Geomatica 2013 software was used. The

310 DEM was derived using the Rational Function model with first-order RPC adjustments from ephemeral data and GCPs. We applied the Wallis filtering to locally enhance the contrast of the image to improve the image matching. The DEM derived from the forward- and backward-looking images has a resolution of 2 m.

In the next step, DEM areas with low quality were removed. First the SRTM-3 DEM and the GeoEye-1 DEM were resampled from 90 to 30 m, and from 2 to 5 m, respectively, and aligned to a raster grid of same extent and cell alignment. Then the

315 noises in the GeoEye-1 DEM were eliminated applying the expand-sink-expand tool and a median filter (5 x 5 m). With the hillshade of the GeoEye-1 DEM we visually checked the DEM. To evaluate the image matching, PCI produces a so-called score channel image, which we used to identify DEM areas of poor quality and set the values to "no data". Especially a small part of the north-eastern glacier area at Yala ridge had to be discarded due to a very low DEM quality.

In the DEM co-registration process, the SRTM-3 is the reference (master) DEM to which the Geoeye-1 slave DEM is co-

320 registered. For the horizontal DEM co-registration, first we calculated the elevation difference of the GeoEye-1 DEM relative to the SRTM-3. We excluded non-stable terrain such as glaciers and landslide areas and use only terrain with a slope between 10° and 45° in SRTM-3. The SRTM-3 had initially a much coarser resolution than the GeoEye-1 DEM, leading to a resolution-induced bias at topographic extremes with strong curvature (Berthier et al. 2006; Paul, 2008; Gardelle et al., 2012). To account for such curvature effects and most extreme outliers in particular at steep slopes, we identified and removed DEM difference

325 values in the 5% and 95% quantiles, as well as pixels outside the two-tailed 1.5 times interquartile range (Pieczonka et al., 2013). The horizontal shift between the two DEMs we corrected manually due to the small study area, followed by a two-dimensional spatial trend correction. For the vertical DEM co-registration of the GeoEye-1 DEM, the flat areas less than 10° of the SRTM-3 were used, avoiding steeper terrain with decreasing accuracy in SRTM-3. The DEM2012 was resampled to a resolution of 5 m for the geodetic method and 30 m for the glaciological method.

330 **3.4 Analysis of glacier changes and uncertainties**

**3.4.1 Point and glacierwide mass balance**

The glacier-wide mass balances, ELA and AAR were calculated based on the interpolated mass balance gradient derived from the point measurements following a similar method used by Wagnon et al. (2013).

The point mass balances are easy to calculate where ablation dominates, and are alike for measurements from multiple older

335 stakes at the same location. In the accumulation area the analysis of the point data tends to be difficult because of the above described challenges during data collection. In such cases, each stake and snow pit measurement were assessed, and the main processes ablation and accumulation reconstructed.

The errors of the point measurements were assessed by analysing the random errors for each measurement from density $\sigma_d$, ice surface roughness $\sigma_{rough}$ mainly in the ablation area, varying snow depth $\sigma_{depth}$ mainly in the accumulation area, stake

340 reading $\sigma_{read}$, errors due to the sawdust spread for snow pit measurements $\sigma_{sawd}$ and movement of the stake in the firn area $\sigma_{firn}$. The error of individual point measurement $\sigma_{point}$ was calculated:

$$\sigma_{point} = \sqrt{\sigma_d^2 + \sigma_{rough}^2 + \sigma_{depth}^2 + \sigma_{read}^2 + \sigma_{sawd}^2 + \sigma_{firn}^2} \qquad (1).$$

At few sites with minimal flow, two measurements from older and newer stakes allowed a comparison. In most cases the measurements were within the calculated error. Otherwise, if no explanation was found for differing values, the standard

345     deviation of the two values was taken as error. The error of the point measurements for a specific elevation band
        $\sigma_{point\_elevb}$ was calculated by considering $n$ point measurements in the respective elevation band:

$$\sigma_{point\_elevb} = \sqrt{\sum_{point=1}^{n} \sigma_{point}^2}/\sqrt{n} \qquad\qquad (2).$$

        The mass balance gradients were derived from the regression lines of the point measurements and applied to the DEMs of
        Yala and Rikha Samba glacier. For Yala Glacier, a gradient for the ablation area was identified, and separately analysed for

350     the annual and seasonal mass balances, with the winter and summer season starting in November and May or June, respectively.
        Too few measurements in the accumulation area inhibited to identify a gradient for the accumulation area. For Rikha Samba
        Glacier three characteristic annual gradients were identified, with a large gradient in the ablation area, a medium gradient in
        the transition between ablation and accumulation area, and a very small or no gradient in the accumulation area.

        Based on the assumption that the mass balance gradients remain very similar in different mass balance years, gradients were

355     reconstructed for Rikha Samba Glacier for years with limited point measurements (2012, 2014, and 2015). The intersection
        points of the lower and middle gradients were identified and reconstructed based on a regression line for sections without
        measurements. In the accumulation area, the starting elevation for a gradient of 0 m w.e. (100 m)$^{-1}$ was assumed between 5850
        and 5950 m, based on the measurements and topographical setting. For the mass balance year 1999, the point measurements
        collected by Fujita et al. (2001) were used.

360     To assess the error of the mass balance for elevation bands and the entire glacier, the errors of the point measurements
        $\sigma_{point\_elevb}$ and interpolation method $\sigma_{int}$ were analysed. Due to a lack of updated glacier surface and outline data, the
        reference-surface balance was calculated (Elsberg et al., 2001), and the systematic errors caused by the changing glacier
        geometry were disregarded. Also, the systematic errors caused by stakes placed at unrepresentative locations or even lack of
        point measurements were not evaluated due to a lack of respective information.

365     To calculate the systematic error caused by the interpolation method $\sigma_{int}$, we estimated the maximum difference in mass
        balance for 50 m elevation bands. The standard deviation of this value and the calculated mass balance was assumed as the
        error from the interpolation method.

        The overall error $\sigma_{final}$ for the mass balance for elevation bands and the glacier-wide balance was calculated:

$$\sigma_{final} = \sqrt{\sigma_{point\_elevb}^2 + \sigma_{int}^2} \qquad\qquad (3).$$

370     The error of the cumulative mass balance $\sigma_{cumul}$ for $n$ years was calculated:

$$\sigma_{cumul} = \sqrt{\sum_{years=1}^{n} \sigma_{final}^2} \qquad\qquad (4),$$

        And the error of the mean annual mass balance rate $\overline{\sigma_{cumul}}$ for $n$ years was calculated:

$$\overline{\sigma_{cumul}} = \sqrt{\sum_{years=1}^{n} \sigma_{final}^2}/\sqrt{n} \qquad\qquad (5).$$

        The ELA and AAR were calculated based on the mass balance gradients, whereas for Rikha Samba Glacier the gradient of the

375     mid-section of the glacier was used. The accuracy of the ELA and AAR were estimated based on the variation of the regression
        lines caused by outlying point measurements. For Rikha Samba Glacier the calculation of the ELA and AAR for the years
        2012, 2014 and 2015 were omitted due to the very few measurements.

**3.4.2 Glacier area and length**

        The glacier area of Yala Glacier has been defined based on the GeoEye-1 Image from 15 January 2012, and GPS data of the

380     terminus from 3 November 2012. On the north-west side, the glacier has been separated along the flowline, based on the
        contour line method from the DEM2012. A section detached from the main glacier on the south-east side was excluded. For

the analysis of the geodetic mass balance, the glacier outline is based on the Landsat 7 ETM+ image from February 2000 (Table S3).

The glacier frontal variations of Yala Glacier were analysed with satellite images, maps and field-based data (Table S1, S2, S3). Yala Glacier is very wide and the terminus is not constrained by a valley. Hence it is difficult to identify a central glacier flowline, and the general glacier flow direction was delineated instead. We applied the 'rectilinear box method' described by Lea et al. (2014) and Koblet et al. (2010). In this method an arbitrary rectangular box is drawn along the flowline. Perpendicular to the flowline and at the maximum extent of Hexagon KH-9 1974 glacier outline, a straight arbitrary baseline was drawn. Perpendicular to the baseline and in flow direction, 26 parallel lines at 50 m intervals were drawn to quantify the glacier terminus changes. At each parallel line we measure the frontal variation and averaged the values for the final frontal variation of that period. There are big outliers, and some of the mapped termini were not covered by all 26 parallel lines. Therefore, for the final calculation only 9 parallel lines which cover the lowest parts of the glacier were considered. For Rikha Samba Glacier, the glacier outline was delineated from Rapid Eye images from 25 and 27 April 2010 for the mass balance analysis, and SRTM-1 was used for the mass balance calculation. The frontal variations are quantified along the central glacier flowline that was derived from SRTM-1. The glacier termini are based on Landsat images from 1989, 2001, 2006, 2011 and a dGPS survey from 2013 (Table S1). Uncertainties of glacier termini and outlines are estimated half to one pixel dependent on the quality of the source image or map scale, or according to the dGPS settings and field conditions.

### 3.4.3 Geodetic mass balance calculation

The geodetic mass balance calculation for Yala Glacier is based on the subtraction of the SRTM-3 from the DEM2012 from the years 2000 and 2012, respectively, which results in a map of elevation differences (Δh). Data gaps smaller than 0.01 km$^2$ in the elevation difference map, were filled with a mean filter of surrounding height change (Δh) values. The accumulation and ablation areas were separated by the ELA of 5350 m a.s.l, which is based on field observations and the balanced ELA calculated from the field-based mass balance measurements. Outliers and voids larger than 0.01 km$^2$ occurred only in the accumulation area. The largest data gaps we found at the edge of the glacier at Yala ridge, where fresh snow in the GeoEye-1 image compromised the quality of the DEM2012. However, no plausible statistical value could replace the data voids and outliers, therefore, the mode value from the accumulation area was taken, assuming only minor elevation changes in these areas (Schwitter and Raymond, 1993). Assuming an average density of 850 kg m$^{-3}$ (Huss, 2013) for the entire glacier, the elevation change was converted into mass change. Since the accumulation area was small, only a single density value was used. The glacier area was defined by the larger extent from the Landsat 7 image from February 2000. Additionally, the glacier surface elevation changes of Yala Glacier were analysed along a profile line surveyed by dGPS in May 2012, and compared to SRTM-3.

The SRTM-3 C-band potentially underestimates the glacier elevations because of radar penetration into the upper snow, firn and ice layers on the glacier (Kääb et al., 2012; Gardelle et al., 2012). In winter in the Karakoram, Gardelle et al. (2012) found a penetration on glacier of a couple of metres below 5300 m, which increases to about 5 m at 5700 m and more above. They emphasise that these values can vary in different regions, decreasing penetration in wetter and warmer snow and dirtier ice. Bolch et al. (2016) use a mean average penetration correction of 2.4 ±1.4m to address this issue in the Karakoram. The Landsat 7 image from February 2000 showed some snow cover. In this study, we assume that the SRTM-3 DEM represents the glacier surface from early 2000 because we expect on average only a small snow cover. Additionally, the accumulation area on Yala Glacier is small and on low elevation, reducing the effect of the penetration.

To assess the uncertainty of the geodetic mass balance calculation, we estimated the vertical DEM precision by calculating the normalized median absolute deviation (NMAD), which is 7.4 m, following the method by Holzer et al. (2015), and considering the density deviation of ±60 kg m$^{-3}$ (Huss, 2013). Errors due to different spatial scale, sensors, resolutions and area of Yala glacier are not considered.

## 4 Results

### 4.1 Mass balances, ELA, AAR and gradients

The glacier-wide annual mass balances of Yala and Rikha Samba Glacier were negative for all years, except in 2013 when Yala Glacier was almost in balance (-0.01 ±0.29 m w.e.), and Rikha Samba Glacier had a slightly positive balance (0.12 ±0.32 m w.e.), reported in Table 2 and 3, Fig. 2, 3 and 4. The most negative annual balances on Yala Glacier occurred in 2015 and 2017 with -1.18 ±0.26 m and -1.18 ±0.20 m w.e. In 2015, a very negative summer balance, overcompensated the very positive winter balance with extraordinary snowfall (Fujita et al., 2017). On Rikha Samba Glacier, 2012 was the most negative year (-0.72 ±0.34 m w.e.), followed by 2015 (-0.63 ±0.35 m w.e.). During the Nepal earthquakes in April and May 2015, Langtang was heavily affected by ice avalanches, landslides, and as well as rockfalls on the glacier in the immediate vicinity of the study area (Kargel et al., 2016, Fujita et al., 2017). Direct effects of the earthquake on the glacier could not be measured, however the climate station on and near the glacier were destroyed likely because of air blasts from ice avalanches. The effect of the air blasts on the snow cover of Yala Glacier is not known, however, it is possible that snow was blown away and partly sublimated. The air in the valley was filled with dust and it is probable that more dust than usual settled on Yala Glacier, increasing ablation. In the years 2012, 2014 and 2016 the values were similarly negative for the Yala Glacier (-0.86 ±0.40 m, -0.61 ±0.27 m and -0.61 ±0.23 m w.e.). For Rikha Samba Glacier, the balances were similarly negative for the years 2012, 2014 and 2015 (-0.72 ±0.34 m, -0.55 ±0.34 m and -0.63 ±0.35 m w.e.), followed by less negative years in 2016 and 2017 (-0.33 ±0.27 m and -0.23 ±0.31 m w.e.). The most negative point mass balances of -3.75 ±0.05 m w.e. and -4.12 ±0.04 m w.e., respectively, were measured at the lowest stakes (5175 m and 5437 m a.s.l.) of Yala and Rikha Samba Glacier in 2012.

445

**Table 2: Mass balance (B) measured with the glaciological method, winter balance (BW), summer balance (BS), ELA, AAR and mass balance gradient for Glacier from 2011 to 2017.**

| | **Yala Glacier** | | | | | | |
|---|---|---|---|---|---|---|---|
| **B year** | **B (m w.e.)** | **Bw** | **Bs** | **Bw+Bs** | **ELA (m a.s.l.)** | **AAR** | **db/dz (m w.e. (100 m)$^{-1}$)** |
| 1999 | | | | | | | |
| 2012 | -0.86 ±0.40 | 0.16 | -0.20 | -0.03 | 5454 ±30 | 0.28 | 1.14 |
| 2013 | -0.01 ±0.29 | 0.36 | -0.35 | 0.01 | 5380 ±20 | 0.48 | 0.99 |
| 2014 | -0.61 ±0.27 | 0.27 | -0.99 | -0.73 | 5431 ±20 | 0.35 | 1.18 |
| 2015 | -1.18 ±0.26 | 0.54 | -1.12 | -0.59 | 5510 ±40 | 0.13 | 0.90 |
| 2016 | -0.61 ±0.23 | 0.19 | -0.79 | -0.60 | 5444 ±20 | 0.31 | 0.93 |
| 2017 | -1.18 ±0.20 | 0.20 | -1.39 | -1.19 | 5486 ±20 | 0.19 | 1.10 |
| Mean | -0.74 ±0.28 | 0.29 | -0.81 | -0.52 | 5451 | 0.29 | 1.04 |
| STD | 0.44 | 0.14 | 0.46 | 0.45 | 45 | 0.12 | 0.12 |
| 2011–2017 | -4.44 ±0.69 | 1.72 | -4.85 | -3.13 | | | |

450

**Table 3: Mass balance (B) measured with the glaciological method, ELA, AAR and mass balance gradient for Rikha Samba Glacier from 2011 to 2017. We did not calculate the ELA and AAR for Rikha Samba Glacier for 2012, 2014 and 2015 due to the very few data points.**

| | **Rikha Samba Glacier** | | | | |
|---|---|---|---|---|---|
| **B year** | **B (m w.e.)** | **ELA (m a.s.l.)** | **AAR** | **db/dz (m w.e. (100 m)$^{-1}$)** | **db/dz at ELA (m w.e. (100 m)$^{-1}$)** |
| 1999 | -0.18 | 5790 ±50 | 0.49 | 1.27 | 0.25 |
| 2012 | -0.72 ±0.34 | – | – | 1.13 | |
| 2013 | 0.12 ±0.32 | 5724 ±20 | 0.75 | 1.57 | 0.37 |
| 2014 | -0.55 ±0.34 | – | – | 1.36 | |
| 2015 | -0.63 ±0.35 | - | – | 1.48 | |
| 2016 | -0.33 ±0.27 | 5872 ±50 | 0.41 | 1.64 | 0.36 |
| 2017 | -0.23 ±0.31 | 5862 ±50 | 0.54 | 1.89 | 0.46 |
| Mean | -0.39 ±0.32 | 5807 | 0.55 | 1.48 | 0.36 |
| STD | 0.31 | 63 | 0.15 | 0.25 | 0.09 |
| 2011–2017 | -2.34 ±0.79 | | | | |

455
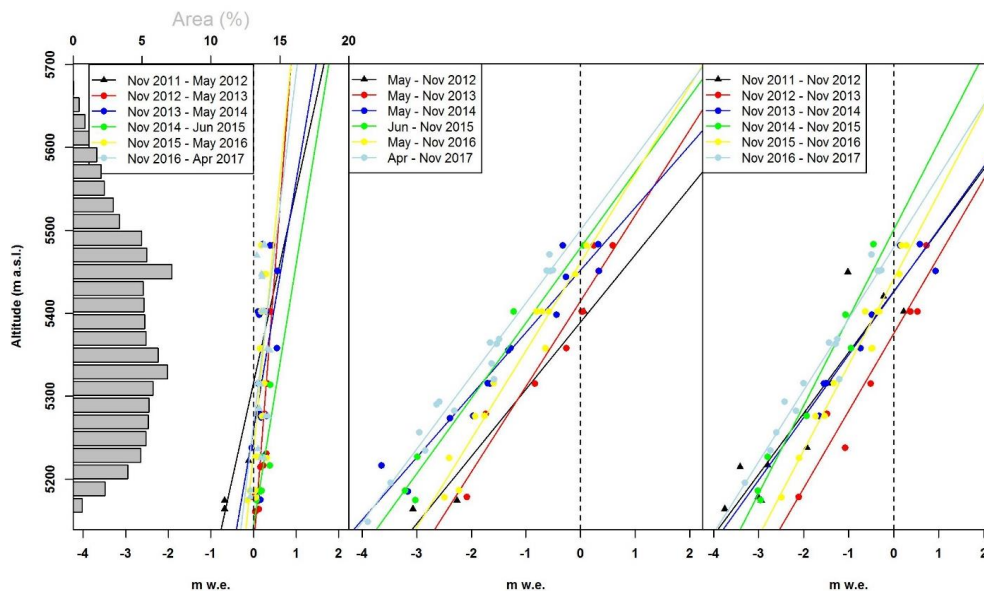
**Figure 2: Mass balance and gradients for the winter (left), summer (right) and annual mass balance for Yala Glacier from 2011–2017, and the glacier hypsography (far left).**
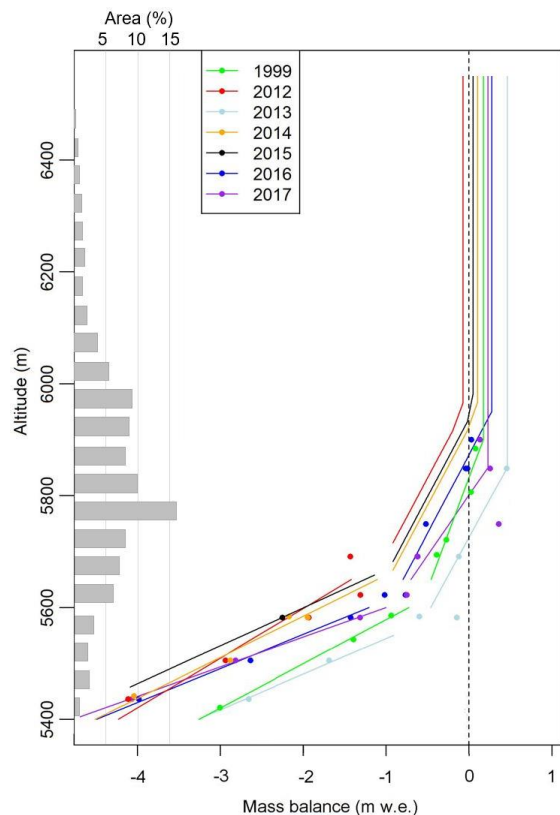
460     **Figure 3: Point mass balance and hypsography of Rikha Samba Glacier for the mass balance years 1999, and 2012 to 2017.**
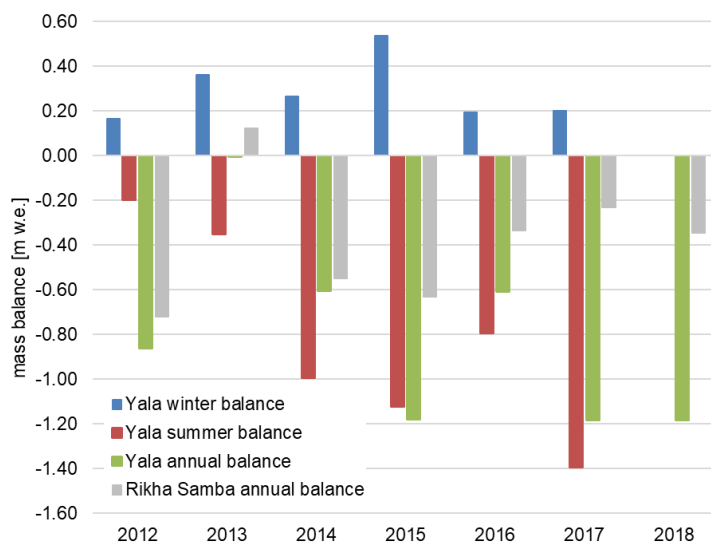
**Figure 4: Winter, summer and annual mass balance of Yala Glacier and annual balance of Rikha Samba Glacier, calculated based on the respective gradients. In the mass balance years 2012 and 2015, the sum of winter and summer balances differ significantly from the annual balances, likely due to a lack of data in higher elevations.**

465    The uncertainties in the accumulation area are larger than in the ablation area because the processes in the snowpack are more complex, influence each other and are difficult to measure. The possible causes for these variations are manifold, from snow/firn compaction, spatial variability of the glacier surface due to varying accumulation and ablation, sawdust promoting local melt, bamboo stakes being pushed up or down and superimposed ice. In some years, the surface roughness was very large in the ablation area, resulting in large errors. Errors for the density of metamorphed snow tended to be larger than for

470    fresh snow because it was harder to measure. At Yala Glacier, the error was largest in the highest elevation bands that make up 15% of the glacier area because the lack of measurements prevented the calculation of a reliable gradient in the accumulation area. Similarly, at Rikha Samba Glacier, the sparse measurements in the accumulation area and in particular in its steep slopes (19 % of the area) resulted in large errors that were difficult to estimate.

At Yala Glacier, the measured average densities with standard deviation for snow and firn were 336 kg m$^{-3}$ ($\pm$81 kg m$^{-3}$) and

475    562 kg m$^{-3}$ ($\pm$128 kg m$^{-3}$). However, harder firn layers were difficult to measure and estimated between 550 kg and 700 kg m$^{-3}$, dependent on the site and firn condition. At Rikha Samba Glacier, the average snow density measured was 399 kg m$^{-3}$ with a standard deviation of $\pm$70 kg m$^{-3}$. For ice we assumed a density of 900 kg m$^{-3}$ (Cogley et al., 2011).

The calculated $ELA_0$ and $AAR_0$ for Yala and Rikha Samba Glacier are 5378 m a.s.l., 5758 m a.s.l., 49% and 66% respectively

480    (Fig. 5). From 2011 to 2017 the ELA ranged at Yala Glacier between 5380 m and 5510 m a.s.l. with uncertainties of ±20 m to

±40 m, and at Rikha Samba Glacier between 5724 m and 5872 m with uncertainties of ±20 m to ±50 m (Fig. 2 and 3, Table 2

and 3). The AAR range from 13% to 48% and from 41% to 75% for Yala and Rikha Samba Glacier, respectively. The snow

line was not a reliable indicator for the ELA, as characteristic for summer accumulation and ablation type glaciers.
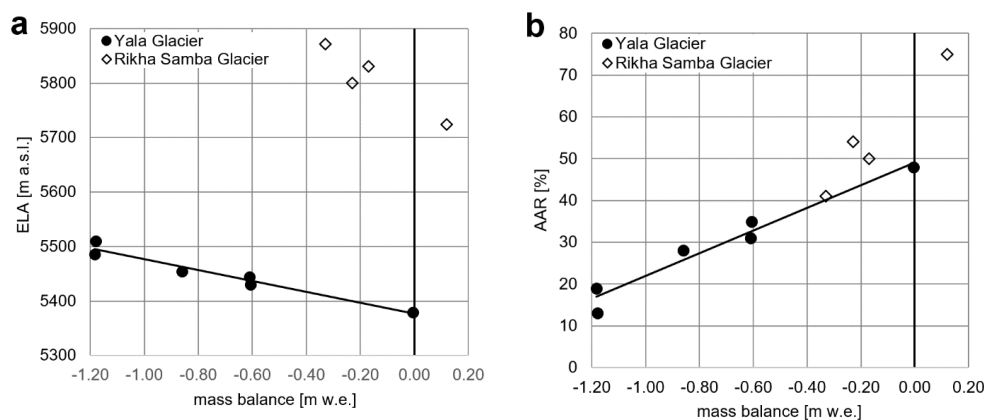
485    **Figure 5: The ELA (a) and AAR (b) of Yala and Rikha Samba Glacier against the mass balance. The ELA0 and AAR0 for the**
**glaciers are 5377 m, 5760 m, 49 % and 66 % for Yala and Rikha Samba Glacier, respectively.**

The point mass balances are shown in Fig. 2 and 3 as function of elevation and with regression lines that are used to derive the

mass balance gradients for Yala and Rikha Samba Glacier, respectively. The mean mass balance gradient at the ELA are

490    1.04 m and 0.36 m w.e. (100 m)$^{-1}$, for Yala and Rikha Samba Glacier, respectively. The gradients are relatively consistent over

the years with standard deviations of 0.12 m and 0.9 m w.e. (100 m)$^{-1}$, respectively. In the lower part of Rikha Samba Glacier,

the gradient is much larger with a mean value and standard deviation of 1.48 m and 0.25 m w.e. (100 m)$^{-1}$. The mass balance

gradients of Yala Glacier are very consistent for the seasonal and annual balance, with only a single gradient observed for the

glacier. Additional measurements in higher elevations likely would have allowed to identify a smaller gradient in the

495    accumulation area. For the winter balance, a small gradient was identified, which is overestimated for years when ablation

already set in on the lower part of the glacier. This is the case for the year 2012 when ablation possibly set in earlier, and 2015

when the stakes were measured a month later than normally, and in both cases without measurements in higher elevations. For

these years, the winter mass balance gradient in the accumulation area is likely smaller than in the ablation area and generally

the mass balance is overestimated above about 5500 m a.s.l.

500    In most years, the winter balances show a slight mass gain on Yala Glacier, which happens mainly from January to May when

snowfall sets in. The average winter balance was 0.29 m w.e. with a standard deviation of 0.14 m w.e. However, in winter

2014/2015 an exceptional amount of precipitation was measured at various climate stations. In that winter local people in

Langtang reported many Yaks dying in the snow, and during the Gorkha Earthquake in April extreme avalanches were

triggered (Fujita et al., 2017). Above average accumulation (0.54 m w.e.) was calculated for the winter 2015 mass balance

505    despite a delay of measurements by a month. However, the uncertainty is higher because of lacking measurements in higher

elevations. The summer balances indicate an average mass loss of -0.81 m w.e. and standard deviation of 0.46 m w.e. In early

October 2013 and 2014, the Central Himalayas received large amounts of precipitation brought by the cyclones Phailin and

Hudhud (Shea et al. 2015b; Necker et al., 2015). These precipitation events in form of snow contributed to the summer balance

since the measurements were taken after the cyclones passed.

510 We identify distinct snow and ice layers only after some winters, such as in April 2017 (Fig. 6). In autumn, often only a very fresh layer of snow was clearly detectable over the entire glacier, and in some years the sawdust marking the previous measurement was removed by ablation before accumulation. Without the sawdust found at the bottom of the snowpits at S6, S7 and S8 the lowest layer of darker coarse snow could be mistaken for snow from the monsoon season. The amount of snow accumulation depended mainly on the elevation, but also aspect, slope and exposure. Maximum accumulation we typically

515 measured at stake 7, which is less exposed than the stakes 6 and 8. In April 2014, we measured superimposed ice, which formed at the glacier surface below the snow from the cyclone Phailin. The cumulated winter and summer balances largely sum up to the annual mass balances, except in 2012 and 2015 when the cumulated winter and summer balances underestimate the annual mass loss by -0.83 m and -0.59 m w.e.
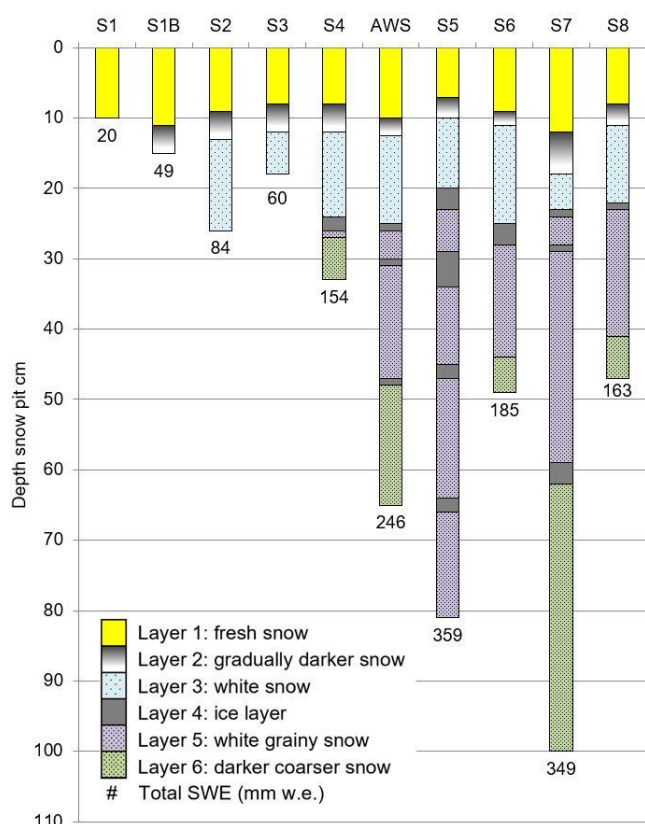
520

**Figure 6: Snow profiles measured at the stakes on Yala Glacier on 23, 24 and 25 April 2017. At the site AWS, a temporary weather station was set up near stake S4. Distinct snow layers can be identified at all measurement sites. At the stakes S5, S6, S7, and S8 sawdust from 19 and 20 November 2016 was found at the bottom of the snow pit and glacier ice at all lower sites.**

525

Earth System
Science
Data

During the twelve-year period (2000–2012) Yala Glacier's average glacier thinning was -10.49 ±7.41 m, with an annual thinning rate of -0.87 ±0.62 m a$^{-1}$, which corresponds to a net mass loss of -8.92 ±6.33 m w.e., and an annual rate of -0.74 ±0.53 m w.e. a$^{-1}$ (Fig. 7, Table 4). The thinning rate along the profile line is higher (-1.1 ±0.13 m a$^{-1}$) but within the uncertainty range of the DEM thinning rate, most likely because accumulation above 5571 m is excluded from the calculation. Maximum 530 thickness gain of 17.63 m was measured below the ice cliffs, and the biggest ice wastage was measured above the lake and along the glacier terminus, with a value of -50.66 m. Positive mass balance values lie in the upper part of the glacier. However, when averaging the values over elevation bands, we see a mass gain only in the highest elevation bands, which is filled with the mode value from the accumulation area (Fig. 8).
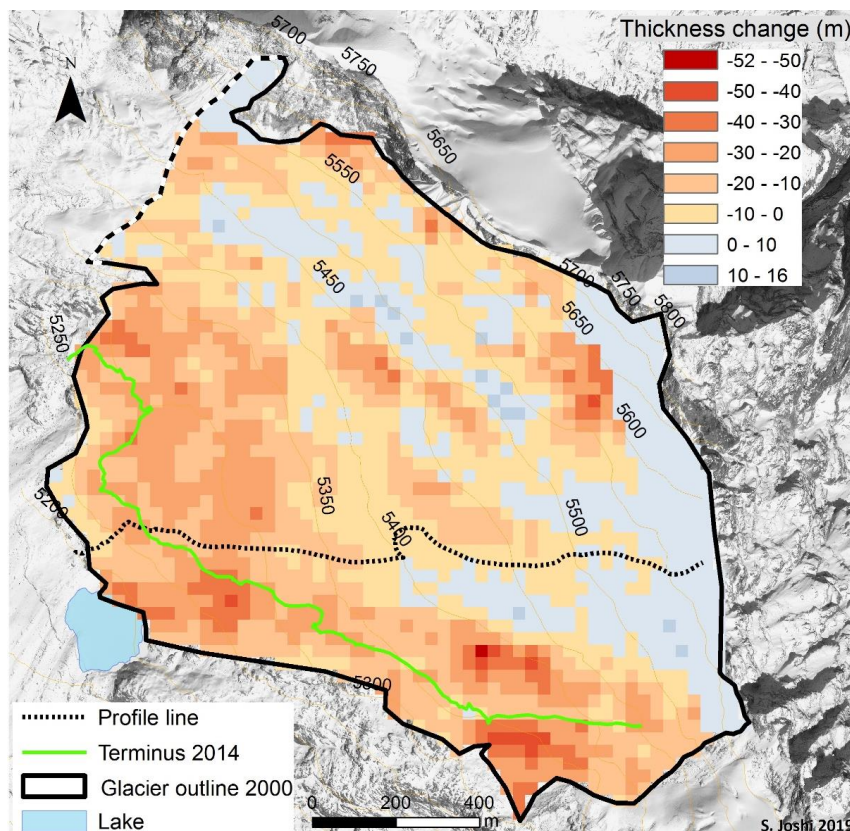
535 **Figure 7: Thickness changes of Yala Glacier in metres after DEM differencing of GeoEye-1 (Jan 2012) and SRTM3 (Feb 2000) DEM and dGPS profile in 2012.**

**Table 4: Comparison of glacier surface lowering and in-situ mass balance measurements from various studies. Conversions of thickness change (\*) calculated assuming a density of 850 kg m-3 and annual uncertainties calculated based on authors' values and**

540 **Zemp et al. (2013).**

| Duration | Total years | Glacier | Annual thickness change (m a⁻¹) | Annual mass balance rate (m we a⁻¹) | Method | Source |
|---|---|---|---|---|---|---|
| 2000–2012 | 12 | Yala | -0.87 ±0.62 | -0.74 ±0.53* | DEM differencing | This study |
| 2000–2012 | 12 | Yala profile | -1.1 ±0.13 | -0.94 ±0.11* | DEM differencing | This study |
| 2011–2017 | 6 | Yala | | -0.74 ±0.28 | Direct measurements | This study |
| 2006–2015 | 9 | Yala | -0.89 ±0.23 | -0.76 ±0.24 | DEM differencing | Ragettli et al., (2016) |
| 2000–2016 | 16 | Yala | -0.52 ±0.21 | -0.44 ±0.18* | DEM differencing | Brun et al., (2017); WGMS 2019 |
| 1996–2009 | 13 | Yala profile | -0.75 ±0.24 | -0.64 ±0.20* | dGPS and GPR Survey | Sugiyama et al., 2013 |
| 1996–2009 | 13 | Yala | | -0.80 ±0.16 | DEM differencing | Fujita and Nuimura, 2011 |
| 2006–2015 | 9 | 7 glaciers in Langtang | -0.45 ±0.18 | -0.38 ±0.17 | DEM differencing | Ragettli et al. (2016) |
| 2000–2016 | 16 | 3 glaciers in Langtang | | -0.58 ±0.08 | DEM differencing | Maurer et al., 2019 |
| 2011–2017 | 6 | Rikha Samba | | -0.39 ±0.32 | Direct measurements | This study |
| 2000–2016 | 16 | Rikha Samba | -0.44 ±0.27 | -0.37 ±0.23* | DEM differencing | Brun et al., (2017); WGMS 2019 |
| 1998–2010 | 12 | Rikha Samba | | -0.48 ±0.10 | DEM differencing | Fujita and Nuimura, 2011 |
| 2011–2017 | 6 | Mera | | -0.31 ±0.17 | Direct measurements | Wagnon et al., 2020 |
| 2011–2017 | 6 | Pokalde | | -0.75 ±0.28 | Direct measurements | Wagnon et al.,2013; WGMS 2019 |
| 2000–2011 | 11 | Everest Region | | -0.26 ±0.13 | DEM differencing | Gardelle et al., 2013 |
| 2000–2008 | 8 | Everest Region | | -0.45 ±0.60 | DEM differencing | Nuimura et al., 2012 |
| 2002–2007 | 5 | Everest Region | | -0.79 ±0.52 | DEM differencing | Bolch et al., 2011 |
| 2002–2014 | 12 | Chhota Shigri | | -0.56 ±0.40 | Direct measurements | Azam et al., 2016 |
| 2000–2016 | 16 | Himalayan glaciers clean | | −0.38 ±0.08 | DEM differencing | Maurer et al., 2019 |
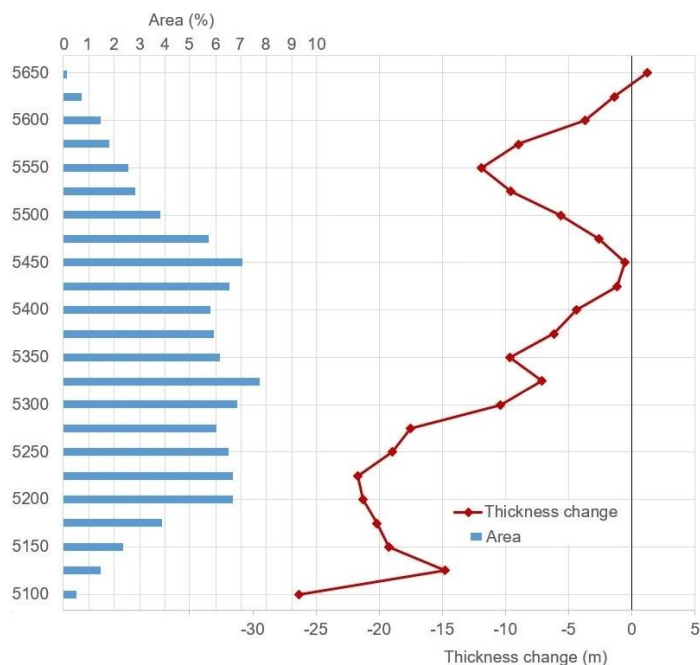
**Figure 8: The mean thickness changes of Yala Glacier for 25 m elevation bands with hypsography, from 2000 to 2012. The reduced thickness change at an elevation of 5125 m is likely a result of the thinner ice thickness in the steeper part of the glacier in 2000. The increased thinning between 5525 and 5575 m a.s.l. might be caused by increased ablation at steep slopes and ice cliffs.**

The annual and cumulative balances of both glaciers show a similar pattern (Fig. 9, Table 2 and 3), however, the mean annual rate and cumulative balance of Yala Glacier from 2011 to 2017 are more negative (-0.74 ±0.28 m w.e. a$^{-1}$, -4.44 ±0.69 m w.e.) than of Rikha Samba Glacier (-0.39 ±0.32 m w.e. a$^{-1}$, -2.34 ±0.79 m w.e). From 2000 to 2017, Yala Glacier lost -12.50 m w.e. with an annual rate of -0.74 ±0.53 m w.e. a$^{-1}$.
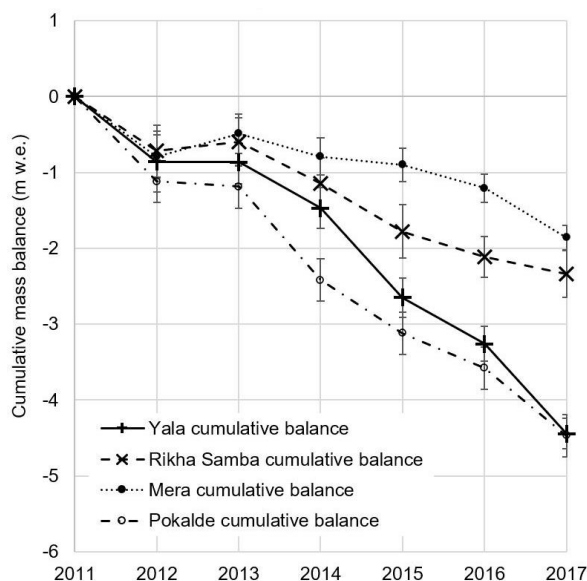
**Figure 9: Cumulative mass balances of Yala, Rikha Samba, Mera and Pokalde Glacier. The data for Mera and Pokalde Glacier is from Wagnon et al. 2013, Sherpa et al. 2017, WGMS, 2020, and Wagnon et al. 2020.**

**4.2 Glacier length changes and flow**

555     The glacier length changes for Yala and Rikha Samba Glacier are reported in Table 5 and displayed in Fig. 10 and 11. Yala Glacier retreated from 1974 to 2016 by -346 m, with an annual rate of -8.2 m a$^{-1}$. The fastest retreat with a rate of -14.1 m a$^{-1}$ happened between 2000 and 2012, when the glacier retreated 169 m over a large rock step behind the lake. The smallest rates of -3.8 m and -3.9 m a$^{-1}$ were measured from 1974 to 1981 and 2014 to 2016. Rikha Samba Glacier showed much larger retreat rates than Yala Glacier, with an average of -18.0 m a$^{-1}$, and a total retreat of -431 m between 1989 and 2013. We measured

560     maximum retreat rates of -31.8 m a$^{-1}$, from 2011 to 2016, when the glacier retreated by -159 m. The smallest retreat rates of -12.4 m a$^{-1}$ were measured during a retreat of 149 m from 1989 to 2001.

**Table 5: Frontal variations of Yala and Rikha Samba Glacier.**

| Time period | Frontal variation (m) | Uncertainty (m) | Annual rate (m a$^{-1}$) | Source |
|---|---|---|---|---|
| **Yala Glacier** | | | | |
| 1974–1981 | -26.9 | ±5 | -3.8 | Hexagon KH-9 / GEN map |
| 1981–2000 | -129.0 | ±31 | -6.8 | GEN map / Landsat 7 |
| 2000–2012 | -169.1 | ±30 | -14.1 | Landsat 7 /dGPS |
| 2012–2014 | -13.0 | ±1 | -6.5 | dGPS / dGPS |
| 2014–2016 | -7.7 | ±1 | -3.9 | dGPS / dGPS |
| **1974–2016** | **-345.8** | **±5** | **-8.2** | Hexagon KH-9 / dGPS |
| **Rikha Samba Glacier** | | | | |
| 1974–1994 | -215.8 | | -10.8 | Fujita et al. 2001 |
| 1994–1998 | -72.8 | | -18.2 | Fujita et al. 2001 |
| 1998–1999 | -11.5 | | -11.5 | Fujita et al. 2001 |
| 1989–2001 | -149 | ±30 | -12.4 | Landsat 4 / Landsat 7 |
| 2001–2006 | -71 | ±30 | -14.2 | Landsat 7 / Landsat 5 |
| 2006–2011 | -159 | ±30 | -31.8 | Landsat 5 / Landsat 5 |
| 2011–2013 | -52 | ±15 | -26.0 | Landsat 5 / dGPS |
| **1989–2013** | **-431** | **±34** | **-18.0** | Landsat 4 / dGPS |
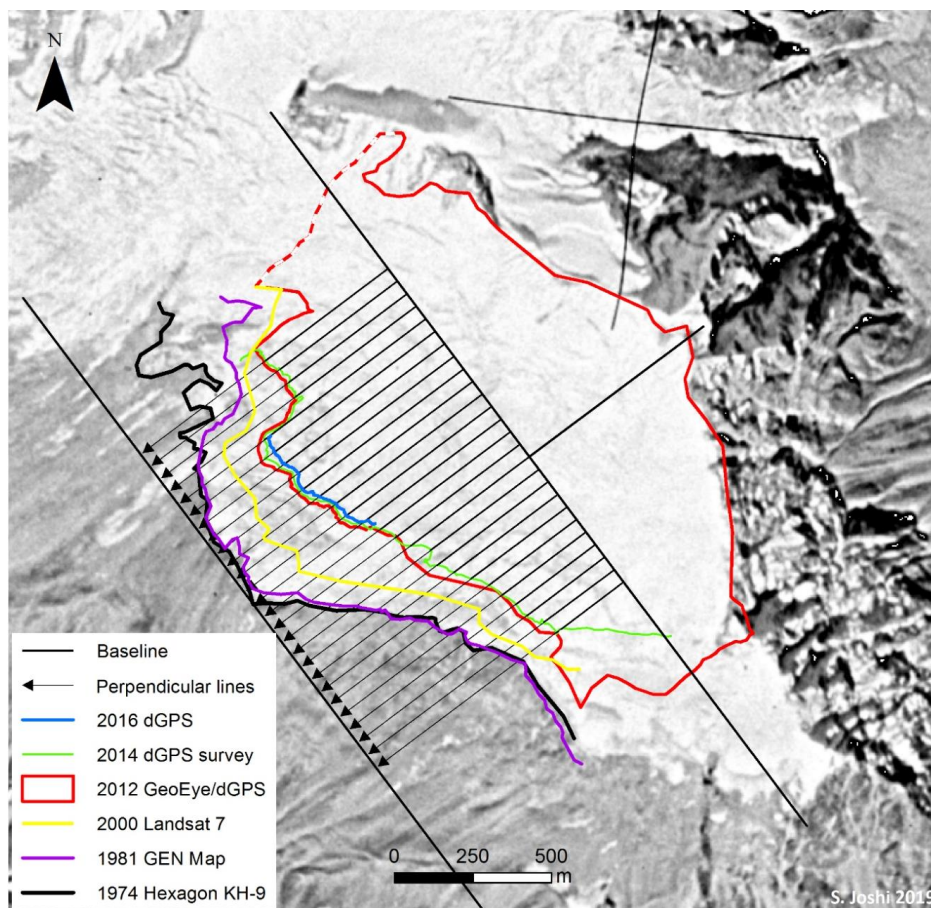
Figure 10: Frontal variations of Yala Glacier from 1974 to 2016. The general flow direction is indicated by a straight black line starting at the highest point of the glacier (north east corner). An arbitrary baseline is at the maximum extent of 1974 (black outline), and 26 parallel arrows in flow direction at 50 m intervals we used to calculate average front variations, but only the 9 bold lines were used for the analysis to exclude outliers. The background image is the Hexagon KH-9 from 1974.
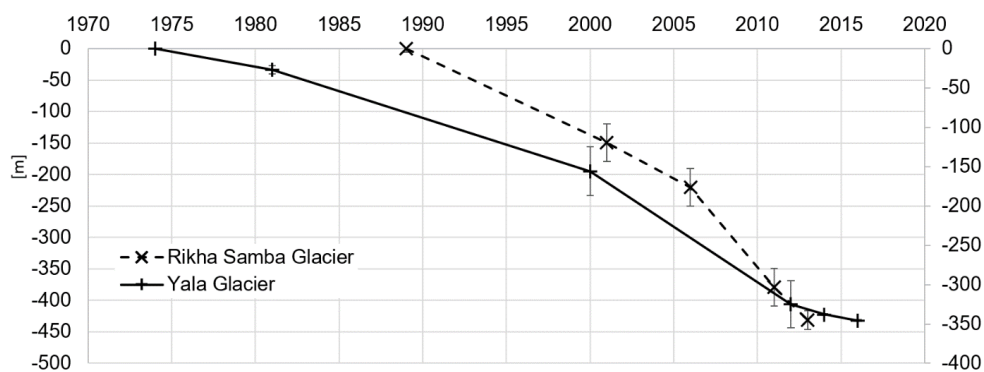
Figure 11: Cumulative glacier retreat of Yala and Rikha Samba Glacier, with uncertainty range.

Glacier flow was measured on Yala Glacier between 8 May 2012 and 5 May 2014. The mean horizontal flow was 5.8
±0.4 m a$^{-1}$, with a minimum and maximum velocity of 4.6 ±0.4 m a$^{-1}$ and 7.8 ±0.4 m a$^{-1}$, respectively (Fig. 12, 13, Table 6).
The glacier surface lowered at each measured stake, on average by 3.4 ±0.4 m a$^{-1}$. While reinstalling stakes in the lowest part
of the glacier, it was observed that flow velocities were typically less than 5 m a$^{-1}$.
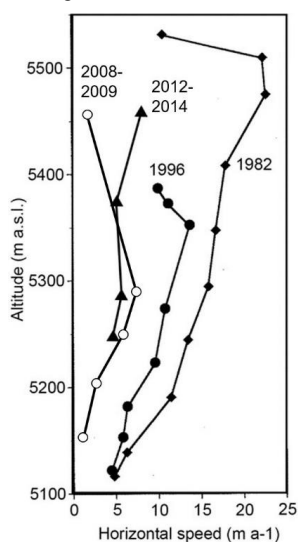
**Figure 12: Altitudinal distribution of the surface flow speeds of Yala Glacier, surveyed in 1982 (solid diamonds, Ageta et al. 1984),
in 1996 (solid circles, Fujita et al. 1998), 2008 to 2009 (open circles, Sugiyama et al., 2013) and from 2012 to 2014 (solid tringle, this
study) (modified Fujita et al. 1998).**
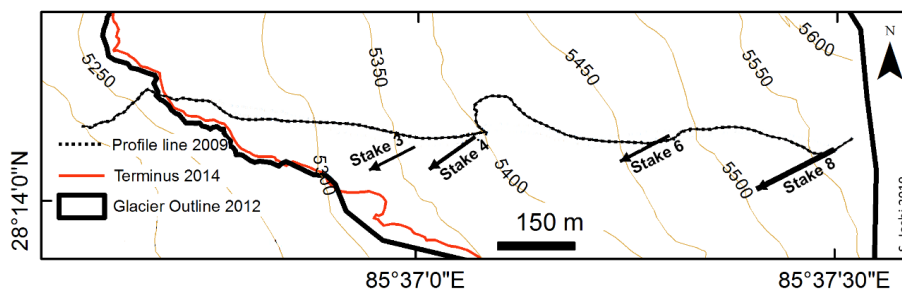
**Figure 13: Glacier flow from 8 May 2012 to 5 May 2014 at the stakes 3, 4, 6 and 8, with annual rates between 4.6 and 7.8 m. The
black arrows show the flow direction and the lengths indicate the annual speed of glacier surface flow, which is depicted 10 times
longer than the real flow. The densely dashed line is the profile line from Sugiyama et al. 2013 (Figure modified from Sugiyama et
al. 2013).**

**Table 6: Glacier flow in metres and direction of Yala Glacier at the stakes S3, S4, S6 and S8 from 8 May 2012 to 5 May 2014.**

| Stake | Horizontal flow (m) | Annual flow (m a$^{-1}$) | Flow direction | Altitude in 2012 | Altitude in 2014 | Vertical flow (m) | Annual (m a$^{-1}$) |
|---|---|---|---|---|---|---|---|
| 3 | 9.1 | 4.6 ±0.4 | S63W | 5249 | 5242 | 7.0 | 3.5 ±0.4 |
| 4 | 11.2 | 5.6 ±0.4 | S56W | 5286 | 5279 | 7.1 | 3.6 ±0.4 |
| 6 | 10.0 | 5.0 ±0.4 | S62W | 5373 | 5366 | 7.1 | 3.6 ±0.4 |
| 8 | 15.6 | 7.8 ±0.4 | S63W | 5457 | 5450 | 6.2 | 3.1 ±0.4 |
| **Average** | | **5.8 ±0.4** | | | | | **3.4 ±0.4** |

## 5 Discussion

### 5.1 Annual glacier-wide mass balances, ELA and AAR

In the Himalayan region various studies observed an accelerated thinning trend over the past decades and heterogeneous thinning patterns (e.g. Maurer et al., 2019; Ragettli et al., 2016; Nuimura et al., 2012; Bolch et al., 2011; Gardelle et al., 2013). For 18 Himalayan glaciers Azam et al. (2018) assessed a mean rate of -0.49 m w.e. a$^{-1}$ for directly measured glacier mass balance for the period from 1975 to 2015. Maurer et al. (2019) calculated a Himalayan-wide geodetic mass balance of −0.38 ±0.08 m w.e. a$^{-1}$ for clean ice from 2000 to 2016. The mass balance rate of Rikha Samba Glacier is within a similar range, however, the one of Yala glacier is more negative. For Chhota Shigri Glacier in the Western Himalaya, Azam et al. (2016) found a mass balance rate of -0.56 ±0.40 m a.s.l. from 2002 to 2014 in direct measurements.

In Nepal, the mean annual mass balance rates of the small low-lying Yala and Pokalde Glacier from 2011 to 2017 are similar (Table 4, -0.74 ±0.28 m and -0.75 ±0.28 m w.e. a$^{-1}$). Rikha Samba and Mera Glacier are both higher lying glaciers with a larger elevation range and smaller mass balance rates (-0.39 ±0.32 m and -0.31 ±0.17 m w.e. a$^{-1}$; Wagnon et al., 2020). These tendencies are reflected in the cumulative mass balances that are negative for Mera and Rikha Samba Glacier, and even more negative for Yala and Pokalde Glacier (Fig. 9). Mera Glacier has the largest elevation range (4940–6420 m a.s.l.) and similar upper limits as Rikha Samba Glacier (5416–6515 m a.s.l.), but a lower ELA$_0$ (~5515 m a.s.l.), and a large accumulation area with an AAR$_0$ of about 0.60. Rikha Samba Glacier has a smaller elevation range (1100 m vs. 1460 m), and a smaller average mass balance gradient at the ELA than Mera Glacier (0.36 m vs. 0.45 m w.e. (100 m)$^{-1}$), which indicates the likely more continental condition on the north side of the Himalayan main divide, opposed to Mera Glacier on the south side of the main divide.

For Rikha Samba Glacier, Fujita and Nuimura (2011) and Brun et al. (2017) calculated mass balance rates of -0.48 m w.e. a-1 (1998–2010) and -0.37 ±0.23 m w.e. a-1 (2000–2016), which are close to the values calculated in this study, however, the time periods vary, and Fujita and Nuimura (2011) largely excluded elevations above 6000 m a.s.l. Fujita and Nuimura (2011) calculated so-called preferable ELAs for the glacier extents of Yala and Rikha Samba in 2009 and 2010, which are 5260 m and 5545 m a.s.l., respectively, and are lower than the calculated ELA$_0$ of 5378 m and 5758 m a.s.l. in this study. Varying glacier areas and elevation ranges are likely reasons for the differences.

For Yala Glacier, Ragettli et al. (2016) calculated a mass balance rate of -0.76 ±0.24 m w.e. a$^{-1}$ from DEM differencing for 2006 to 2015, which is nearly the same as calculated in this study. Fujita and Nuimura (2011) and Sugiyama et al. (2013) calculated mass balance rates of -0.80 ±0.16 m and -0.64 ±0.20 m w.e. a$^{-1}$, respectively, from 1996 to 2009, and Brun et al., (2017) calculated an annual rate of -0.44 ±0.18 m w.e. a$^{-1}$, from 2000 to 2016, which are within the uncertainty ranges but for different time periods. Yala Glacier's annual mass balance rate of -0.74 ±0.53 m w.e. a$^{-1}$ from 2000–2012 is higher than the average rates measured in the Everest Region by Gardelle et al. (2013; 2000–2011: -0.26 ±0.13 m w.e. a$^{-1}$) and Nuimura et al. (2012; 2000–2008: -0.45 ±0.60), and similar to the value calculated by Bolch et al. (2011; 2002–2007: -0.79 ±0.52 m w.e. a$^{-1}$). However, over a region, mass balances can be very heterogeneous. Ragettli et al. (2016) assessed the geodetic mass balances of two clean and five debris-covered glaciers in Langtang and found a very heterogeneous pattern and a mean annual mass balance rate of -0.45 ±0.18 m w.e. a$^{-1}$. Maurer et al. (2019) calculated a median balance of about -0.54 m w.e. a$^{-1}$ for the clean glaciers in the subregion including Langtang, and a mean rate of -0.58 ±0.08 m w.e. a$^{-1}$ for three debris covered glaciers in Langtang from 2000 to 2016, which is a bit more negative than calculated for the same glaciers by Ragettli et al. (2016).

The mass balance bias by low-lying glaciers with a small elevation range is demonstrated by Yala and Pokalde Glacier. Both are small glaciers on a lower altitude with a small elevation range (5168 m–5661 m, and 5430 m–5690 m a.s.l., respectively). Immerzeel et al. (2012), found that from 1957 to 2002 in Langtang 77 % of precipitation fell between June and September, and Ageta and Higuchi (1984) reported about 80 % of the annual precipitation in the same months for east Nepal. Shea et al. (2015b) estimated the height of the 0° C isotherm in Langtang between 3000 m a.s.l. in winter and 6000 m a.s.l. during

monsoon. Hence, the negative balances of the two small glaciers can be explained by the small amount of accumulation during the main precipitation season in monsoon. Yala and Pokalde Glacier likely have a bias towards negative mass balances, like AX010 Glacier in the Shorong Himal, Nepal and are very sensitive to temperature (Fujita and Nuimura, 2011; Ragettli et al., 640 2016). Such bias results in the overestimation of negative mass balances in the region (Gardner et al., 2013). In comparison, Ragettli et al. (2016) calculated a balanced mass budget of -0.02 ±0.13 m w.e. a⁻¹ for the clean Kimoshung Glacier in close vicinity of Yala Glacier about 3.5 km away, and explain the difference with the very different hypsometry. Compared to Yala Glacier, Kimoshung Glacier has a steep tongue and a large accumulation area (AAR of 86%) at high altitude, which is less exposed to air temperatures above 0° C and making the glacier less sensitive to temperature. The accumulation area is possibly 645 sheltered from the strong westerly winter winds by a mountain ridge running from northwest to southeast, reducing ablation by wind and sublimation, but receiving precipitation largely in form of snow. These issues highlight the importance of investigating large glacier elevation ranges, measuring mass balances in the accumulation areas and precipitation data in high altitudes.

On Yala Glacier positive point net balance data from the eighties and nineties are more positive than those measured in this 650 study (Fig. 14), indicating increased temperatures possibly combined with decreasing precipitation. On Yala glacier, positive annual point balances were measured above 5400 m a.s.l. in all years except 2015 and 2017. In the eighties and nineties, Japanese and Swiss researchers measured snow layers with a range of methods. Steinegger et al. (1993) measured deposited snow in a crevasse at 5580 m a.s.l. and identified annual layers from 1981 to 1989 based on the dirt layers, and converted them to water equivalent. Iida et al. (1987) studied snow and dirt layer formation processes, analysed a snow profile at 5333 m a.s.l. 655 and used precipitation data to assign clean and dirt layers to specific periods in the mass balance years 1983 and 1984. Ozawa and Yamada (1989) and Yamada (1991) evaluated snow profiles from various elevations to calculate the net balance from the mass balance years 1986 and 1987, and Yoshimura et al. (2006) retrieved an ice core at 5350 m a.s.l. and identified annual layers from 1984 to 1994 with help of snow algae. Shiraiwa et al. (1992) analysed snow profiles at various elevations, identified surface balances from monsoon 1990 and the following winter balance up to May 1991. Even though the measurements are 660 difficult to compare because of varying methodologies, it can be seen that accumulation was highest in the eighties, and also measured at lower elevations. In the nineties the accumulation decreased, however, accumulation was still measured at elevations where in this study no positive balances were measured. The authors of the earlier studies identified annual layers with confidence, and only Iida et al. (1987) discussed additional dirt layers formed after strong winter snowfall events. In this study the accumulation measurements were challenging because often sawdust layers were gone or older layers hard to assign. 665 In the winter snow at Yala Glacier, we often observed white and grey snow layers, with ice lenses or layers in between (Fig. 6). The ice layers and lenses, superimposed ice and occasional ice fingers indicated melt and refreezing processes, which likely already start in March when incoming solar radiation and temperature increase and April when solar radiation is close to its maximum (Takahashi et al., 1987a; Shea et al., 2015b). Snow from monsoon was usually more metamorphed with darker and coarser grains. Watanabe et al. (1984) reported from April to June melting up to at least 5500 m a.s.l., and an abundance of 670 water from rain and melt in the temperate accumulation area during the Himalayan Glacier Boring Project 1981–1982, which promotes the snow metamorphosis process. In some years we observed icicles hanging from distinct layers in ice cliffs, indicating melt and refreezing processes and impermeable ice layers in the snowpack. Overall, it was challenging to identify annual snow accumulation without help of sawdust layers. The decreased accumulation over the past decades is likely due to the raising temperatures, possibly a decrease in precipitation as observed in the Everest region by Salerno et al. (2015). On the 675 south slopes of Mt. Everest above 5000 m a.s.l., they found that the minimum temperature increased outside of the monsoon season and liquid precipitation decreased significantly from 1993 to 2013. Provided this also applies to other parts of the Central Himalaya, the impact of reduced snowfall could possibly contribute to a large degree to the negative mass balances of Yala, Rikha Samba and other glaciers.
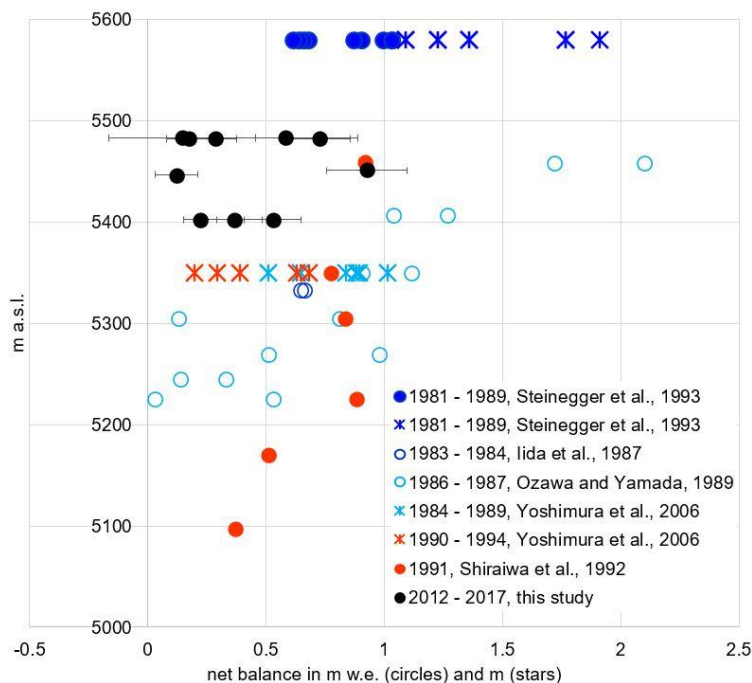
**Figure 14: Positive point net balances in the accumulation area from mass balance years in the 1980ies (blue), 1990ies (red) and from this study (black). The data has been compiled from annual snow pit measurements, multiannual snow profiles, ice cores and crevasses, using dirt, algae or ice layers to distinguish annual layers. Most measurements were converted into water equivalents (circles), and some are only available as snow depth (stars).**

The downwasting of Yala Glacier compromised the consistent representativeness of stake measurements at several locations. For example, between stakes S1 and S1B and near S5, Yala Glacier has very concave surfaces with bowl-shaped areas and transitions to steep slopes. Here the ablation is likely enhanced because of the reflection of radiation (Hock, 2005). Since 2011 onwards, we observed that concave shapes have become more pronounced, ice velocities decreased generally, and the glacier surface downwasted as observed at other glaciers (Ragettli et al., 2016; Sommer et al. 2020). The decreased ice velocities are likely a consequence of the downwasting. At some locations the glacier surface topography changed to a degree that the stake had to be shifted. These small-scale spatial variabilities could cause a bias, which might be later reduced with help of complementing geodetic surface analyses.

The ice cliffs of Yala Glacier are mainly oriented southwest, and slopes steeper than 50° make up approximately 5 % of the map view glacier area and occur over the entire glacier range. Already Ageta et al. (1984) described the ice cliffs and old photos document part of the glacier terminus as ice cliff, at time with an apron (Shiraiwa, 1993). The effect of vertical ablation through melt, sublimation and ice breaking off could be substantial, as observed at glacier ice cliffs in the Antarctic McMurdo Dry Valleys (Chinn, 1987; Lewis et al., 1999), on Kilimanjaro (Winkler et al., 2010), and debris-covered glaciers (e.g. Sakai et al., 2002; Steiner et al., 2015). Ice cliff ablation cannot be quantified with the conventional glaciological method and might lead to underestimating ablation. With geodetical thickness change analyses based on high resolution surface elevations for the entire glacier area the effect could be quantified (Joerg and Zemp, 2014). The mass balance measurements of Yala Glacier are likely and largely representative for comparable slopes in Nepal. However, the mass balance of clean glaciers' ice cliffs remains unknown. While more than 50 % of the glacier area in Nepal is oriented southwest, south, or southeast, less than 1 % of the map view area are slopes steeper than 50° (Bajracharya et al., 2014). Yet, the steeper the ice slopes the smaller is the

surface area in a DEM, hence the surface area of Nepal's ice cliffs and steep ice slopes is underrepresented in such DEM
705     analyses.

**5.2 Seasonal mass balance**

Yala Glacier is considered a summer-accumulation type glacier (Acharya and Kayastha, 2018), and the summer balance
determines the annual balance. However, we measured positive mass balances for every winter season, and only little or no
accumulation in higher elevations during summer (Fig. 2, 4 and Table 2). Fujita et al. (1997b) point out that winter precipitation
710     is more important in Langtang than in Khumbu, which is confirmed by the climate station data described by Shea et al. (2015b)
and could partly explain the winter accumulation. Shiraiwa (1993) highlights the influence of both the summer monsoon and
westerly winter circulation on the annual balance. Wagnon et al. (2013) address the high wind speeds from westerly winds
associated with the jet stream at Mera Glacier (5360 m a.s.l on glacier station) in winter, which causes in combination with
sublimation a substantial part of the winter ablation. Stitger et al. (2018) and Litt et al. (2019) assessed sublimation on Yala
715     Glacier and confirm its strong ablating influence, especially during in favourable conditions such as high wind speed, low
atmospheric vapour pressure and low near-surface vapour pressure. The study of Shea et al. (2015b) shows similarly high
winter wind speeds at Rikha Samba Glacier (5310 m a.s.l, off-glacier station) as at Mera Glacier, but at Yala Glacier
(5060 m a.s.l., off-glacier station) only slightly higher wind speeds than on annual average. It seems reasonable that wind and
sublimation are important ablation processes for Rikha Samba Glacier in winter. At Yala Glacier, in winter when accumulation
720     dominates over ablation the effect of wind and sublimation is probably smaller compared to Mera and Rikha Samba Glacier.
Derived from precipitation data from the Indian Embassy and the Airport in Kathmandu, Seko and Takahashi (1991) found
that winter precipitation (October–April) exceeds summer precipitation (May–September) during 10 years in the period from
1911 to 1986. Salerno et al. (2015) found increased winter temperatures and decreased precipitation above 5000 m a.s.l. in the
Everest region. Additionally, the interannual variability of winter precipitation is much larger than of summer precipitation,
725     which is explained by post-monsoon cyclones and passage of western disturbances with sometimes large amounts of snowfall.
This variability has a significant effect on the mass balance of glaciers in the Nepal Himalaya (Seko and Takahashj, 1991).
Since 1985, the interannual variability was largest in the month of October (Fujita et al., 1997b) and extreme snowfall has been
reported from cyclones in October for several years, such as in 1985 (Seko and Takahashi, 1991; Iida et al., 1987), Phailin in
2013 (Shea et al., 2015b), Hudhud in 2014 (Neckel et al., 2015), and the 1995 India cyclone in November 1995 (Kattelmann
730     and Yamada, 1996). Early or large amounts of winter snowfall protect the glacier longer from ablation by the high albedo. In
winter 2014/15, the exceptional amounts of precipitation likely dampened the effects of the extremely negative summer
balance with less than average precipitation. Still there are only few seasonal mass balance measurements in the Himalayas
and many studies have the main focus on ablation processes. Certainly, the glaciers, especially in humid climates are more
sensitive to temperature changes. However, it would be useful to better understand the impact of the highly variable winter
735     precipitation on the winter balance. For the next few decades such winter accumulation could be important for the survival of
low-lying glaciers and are important contributors for water from snow cover in pre-monsoon.

**5.3 Frontal variation and flow**

On Rikha Samba Glacier, Fujita et al. (2001) measured a retreat of 216 m from 1974–1994 with the slow retreat of -10.8 m a[-1]
(Table 5). From 1994–1998 the glacier retreated 73 m with an accelerated rate of -18.2 m a[-1], followed by a decreased rate.
740     From 2006 to 2011 and 2013 the terminus retreated rapidly 159 m and 52 m, with rates of -31.8 m a[-1] and -26.0 m a[-1],
respectively.
At Yala Glacier, Ono (1985) dated LIA moraines and documented annual ice push moraines, and Yamada et al. (1992) and
Kappenberger et al. (1993) observed terminus retreat since the 70ies with a minor advance in the early 80ies and stagnation,
respectively, followed by continuous retreat. Fujita et al. (1998) noted an accelerated shrinkage in the 90ies, which continued

745 from 2000 to 2012 with a rate of -14.1 m a$^{-1}$ when the glacier retreated over a steep rock step from about 5100 m to 5175 m a.s.l.
From 2012 to 2016 Yala Glacier retreated with an annual rate of -5.2 m a$^{-1}$ in mostly flat terrain, partly in shallow water.
Horizontal flow was also measured with a theodolite from 28 September to 27 October 1982 (Ageta et al., 1984), and from 22
May to 7 October 1996 (Fujita et al., 1998) and a decreasing velocity was observed (Fig. 12). In both studies, the annual flow
rate was assumed to be the same as for the measurement periods, despite varying seasons. Sugiyama et al. (2013) measured

750 the top three stakes on 26 September 2008 and 31 October 2009, and the lower two stakes for four days from 31 October to 4
November 2009 with a dGPS, which were presumably extrapolated to calculate the annual rate, assuming a constant flow. The
flow velocity and direction measured in this study from 2012 to 2014 compares to the measurements from 2008 to 2009.
However, the glacier is slower than in the 80ies and 90ies, and the direction slightly varied, as already shown by Sugiyama et
al. (2013).

755 **6 Conclusions**

Both Yala and Rikha Samba Glacier have been continuously shrinking and retreating in the last couple of decades. The geodetic
mass balance of Yala Glacier showed mass loss of -10.49 ± 7.41 m w. e. from 2000-2012, and an annual rate of -0.74 ±0.53
m w.e. a$^{-1}$, which indicates an unfavourable climate for the glacier. The glacier retreat of 346 m from 1974 to 2016 indicates
that this unfavourable climate trend persisted in the preceding decades. Yala Glacier is not in balance with the climate, and a

760 modelling study by Fujita and Nuimura (2011) confirms that Yala Glacier will likely continue shrinking and retreating in the
coming decades.
At Yala Glacier, the annual balance is determined by the summer balance, however, positive balances were measured in all
winters. A better understanding of the mass balance processes and highly variable precipitation in winter would help to better
understand the water regulating function of glaciers, especially for the many smaller glaciers in lower altitude ranges in the

765 Central Himalayas. This study also confirms the bias towards negative mass balances for small glaciers in lower elevation
ranges. There are no accumulation measurements above 5500 m a.s.l. and thus, no gradient could be identified, and balances
are likely slightly overestimated. Additional accumulation measurements in higher elevations are challenging but would be
useful, to limited degree with snow pits, but for example also terrestrial laser scanning or unmanned aerial vehicles. Vertical
ablation at the steep and mainly southwest facing slopes and ice cliffs could not be quantified, but possibly play a role for the

770 glacier-wide mass balance. Once better data for DEM generation are available especially from laser scans (Joerg and Zemp,
2014), the geodetic mass balance of the entire glacier should be analysed to identify the systematic bias, e.g. caused by steep
slopes and cliffs, or accumulation above 5500 m, and possibly improve the uncertainty assessment. Generally, the surface
topography of Yala Glacier has changed a lot between 2011 and 2017 and very small ice flow velocities were measured. Over
the course of the years, most of the stakes could not be reinstalled at the original coordinates, either because of new crevasses,

775 or significant changes of the surface features at the original site. These are strong indications for the glacier downwasting and
changed glacier characteristics. In an attempt to keep the glacier monitoring going for the next decades, we installed four new
stakes at locations with possibly larger ice thicknesses. An updated high-resolution DEM would do better justice to the changed
glacier topography, and a repeated GPR survey might be beneficial to quantify the remaining ice volume.
In the coming years, ideally distributed physically based mass balance models are developed for both glaciers to improve the

780 annual glacier-wide mass balance calculation. The model likely would use a classic energy balance approach and could be
calibrated and corrected based on the direct and geodetic measurements. Ideally, it would take into account the increased melt
at steeper, exposed areas, and increased deposition of snow in flatter, sheltered areas at Yala Glacier.
The long-term glacier monitoring of Rikha Samba Glacier is very important because of its larger and higher elevation range,
which ensures the survival of the glacier, opposed to Yala Glacier. The processes on Rikha Samba Glacier are not yet well

785 understood. However, winter ablation by wind and sublimation are likely important processes, similar to Mera Glacier.

As the next obvious step, the glacier mass balances should be compared to climatic data. We tried to compare the mass balances from the summer and winter seasons with climate station data, however, because of the data gaps it was impossible. Reanalysis data that have been downscaled with field-based data would be most suitable for that purpose.

790 The Langtang Valley is a well investigated study catchment with multiple types of measurements and monitoring stations. There are several datasets from automatic weather and hydrological stations from various time periods, however, with many gaps due to the challenging environment. The systematic homogenisation of the climatic data according to WMO standards would be beneficial for the assessment of climate reanalysis data, and local, regional and global modelling analyses of e.g. glacier mass balances or runoff.

795 We recommend future complementing geodetic mass balance measurements as part of standard glacier monitoring programmes, which also help addressing systematic errors (Zemp et al., 2013). The development of distributed physically based modelling approaches would improve interpolation for glacier wides mass balance, which likely will result in a reanalyse of the reported mass balance data. More mass balance measurements are needed in accumulation areas, and generally on glaciers with large elevation ranges. These data should be complemented with climate and in particular precipitation data from high elevations, with a focus on precipitation variability and patterns outside the monsoon season to better understand precipitation trends, the impact for low lying glaciers and runoff in the pre-monsoon season. Homogenised climate data would support these efforts.

### Data availability

The data have been submitted to the World Glacier Monitoring Service, is available from the Fluctuations of Glaciers Database http://dx.doi.org/10.5904/wgms-fog-2020-08 (WGMS, 2020a) and is published in the Global Glacier Change Bulletin No. 3 805 (2016–2017) World Glacier Monitoring Service, Zurich, Switzerland (WGMS, 2020b). The Supplement contains additional information related to this article.

### Contributions

DS designed the study and monitoring programme, collected and analysed data, and wrote the manuscript as main author. SPJ collected data and analysed the geodetic mass balance, velocities and frontal variations, and wrote the respective sections. 810 TRG and GS collected and analysed the in situ mass balance and contributed to text editing.

### Competing interests

The authors declare that they have no conflict of interest

### Acknowledgements

We would like to thank the Government of Norway for supporting and funding this research, as well as our national partners, 815 including the Department of Hydrology and Meteorology, Kathmandu University, and Tribhuvan University. This study was partially supported with core funds of ICIMOD contributed by the governments of Afghanistan, Australia, Austria, Bangladesh, Bhutan, China, India, Myanmar, Nepal, Norway, Pakistan, Switzerland, and the United Kingdom. Thanks to all field assistants, trainees and the Trekking Agencies Glacier Safari Treks, Guides for all Seasons and Himalayan Research Expeditions for their support for the glacier measurements and logistic support. We thank Koji Fujita very much for support 820 and dGPS Magellan ProMark 3 data from May 2012, and the GEN map of Yala Glacier. Thanks to Joe Shea, Inka Koch and Santosh Nepal from ICIMOD and Suresh C. Pradhan from DHM for providing temperature and precipitation data of Langtang

area and Kyangjing station. We thank Christa Stephan for providing the orthomap of Langtang, and Pushpalal Ball from the Department of Survey for help to digitize existing topographic data and maps. We thank Tino Piecozonka, Nicolai Holzer and Tobias Bolch for the training and support on the geodetic mass balance analysis, and we thank Patrick Wagnon for his support
825    and advice and reviewing an earlier version of the paper. We thank Matthias Huss for his support for the uncertainty assessment of the glaciological measurements, and Martin Hoelzle for reviewing the article thoroughly.

## References

Abdullah, T., Romshoo, S. A., and Rashid, I.: The satellite observed glacier mass changes over the Upper Indus Basin during 2000–2012, Sci. Rep., 10, 14285, https://doi.org/10.1038/s41598-020-71281-7, 2020.

830    Acharya, A. and Kayastha, R. B.: Mass and Energy Balance Estimation of Yala Glacier (2011–2017), Langtang Valley, Nepal, Water, 11, https://doi.org/10.3390/w11010006, 2019.

Ageta, Y. and Higuchi, K.: Estimation of Mass Balance Components of a Summer-Accumulation Type Glacier in the Nepal Himalaya, Geogr. Ann. Ser. A Phys. Geogr., 66, 249–255, https://doi.org/10.1080/04353676.1984.11880113, 1984.

Ageta, Y., Hajime, I. A., and Watanabe, O.: Glaciological Studies on Yala Glacier in Langtang Himal, Bull. Glaciol. Res., 2, 835    41–47, 1984.

Azam, M. F., Wagnon, P., Ramanathan, A., Vincent, C., Sharma, P., Arnaud, Y., Linda, A., Pottakkal, J. G., Chevallier, P., Singh, V. B., and Berthier, E.: From balance to imbalance: a shift in the dynamic behaviour of Chhota Shigri glacier, western Himalaya, India, J. Glaciol., 58, 315–324, https://doi.org/10.3189/2012JoG11J123, 2012.

Azam, M. F., Wagnon, P., Vincent, C., Ramanathan, A., Linda, A., and Singh, V. B.: Reconstruction of the annual mass 840    balance of Chhota Shigri glacier, Western Himalaya, India, since 1969, Ann. Glaciol., 55, 69–80, https://doi.org/10.3189/2014AoG66A104, 2014.

Azam, M. F., Ramanathan, A.L., Wagnon, P., Vincent, C., Linda, A., Berthier, E., Sharma, P., Mandal, A., Angchuk, T., Singh, V. B., and Pottakkal, J. G.: Meteorological conditions, seasonal and annual mass balances of Chhota Shigri Glacier, western Himalaya, India, Ann. Glaciol., 57, 328–338, https://doi.org/10.3189/2016AoG71A570, 2016.

845    Azam, M. F., Wagnon, P., Berthier, E., Vincent, C., Fujita, K., and Kargel, J. S.: Review of the status and mass changes of Himalayan-Karakoram glaciers, J. Glaciol., 64(243) 61–74, https://doi.org/10.1017/jog.2017.86, 2018.

Bajracharya, S. R., Maharjan, S. B., Shrestha, F., Bajracharya, O. R., and Baidya, S.: Glacier status in Nepal and decadal change from 1980 to 2010 based on Landsat data, ICIMOD, Kathmandu, Nepal, 2014.

Baral, P., Kayastha, R.B., Immerzeel, W.W., Pradhananga, N.S., Bhattarai, B., Shahi, S., Galos, S., Springer, C., Joshi, S.P., 850    and Mool, P.K.: Preliminary results of mass-balance observations of Yala Glacier and analysis of temperature and precipitation gradients in Langtang Valley, Nepal, Ann. Glaciol., 55, 9–14, https://doi.org/10.3189/2014AoG66A106, 2014.

Berthier, E., Arnaud, Y., Vincent, C., and Rémy, F.: Biases of SRTM in high-mountain areas: Implications for the monitoring of glacier volume changes, Geophys. Res. Lett., 33, L08502, https://doi.org/10.1029/2006GL025862, 2006.

Berthier, E., Arnaud, Y., Kumar, R., Ahmad, S., Wagnon, P., and Chevallier, P.: Remote sensing estimates of glacier mass 855    balances in the Himachal Pradesh (Western Himalaya, India), Remote. Sens. Environ., 108, 327–338, https://doi.org/10.1016/j.rse.2006.11.017, 2007.

Bolch, T., Buchroithner, M., Pieczonka, T., and Kunert, A.: Planimetric and volumetric glacier changes in the Khumbu Himal, Nepal, since 1962 using Corona, Landsat TM and ASTER data, J. Glaciol., 54, 592–600, https://doi.org/10.3189/002214308786570782, 2008.

860    Bolch, T., Pieczonka, T., and Benn, D. I.: Multi-decadal mass loss of glaciers in the Everest area (Nepal Himalaya) derived from stereo imagery, The Cryosphere, 5, 349–358, https://doi.org/10.5194/tc-5-349-2011, 2011.

Bolch, T., Kulkarni, A., Kääb, A., Huggel, C., Paul, F., Cogley, J. G., Frey, H., Kargel, J. S., Fujita, K., Scheel, M., Bajracharya, S., and Stoffel, M.: The state and fate of Himalayan glaciers, Science, 336, 310–314, https://doi.org/10.1126/science.1215828, 2012.

865   Bolch, T., Pieczonka, T., Mukherjee, K., and Shea, J.: Brief communication: Glaciers in the Hunza catchment (Karakoram) have been nearly in balance since the 1970s, The Cryosphere, 11, https://doi.org/10.5194/tc-11-531-2017, 531–539, 2017.

Bookhagen, B. and Burbank, D. W.: Toward a complete Himalayan hydrological budget: Spatiotemporal distribution of snowmelt and rainfall and their impact on river discharge, J. Geophys. Res., 115, F03019, https://doi.org/10.1029/2009JF001426, 2010.

870   Brun, F., Berthier, E., Wagnon, P., Kääb, A., and Treichler, D.: A spatially resolved estimate of High Mountain Asia glacier mass balances from 2000 to 2016. Nature Geosci 10, 668–673, https://doi.org/10.1038/ngeo2999, 2017.

Chinn, T. J. H.: Accelerated ablation at a glacier ice-cliff margin, Dry Valleys, Arct. Antarct. Alp. Res., 19, 71–80, https://doi.org/10.1080/00040851.1987.12002579, 1987.

Cogley, J. G., Kargel, J. S., Kaser, G., and van der Veen, C. J.: Tracking the source of glacier misinformation, Science, 327(5965), 522, https://doi.org/10.1126/science.327.5965.522-a, 2010.

875

Cogley, J. G., Hock, R., Rasmussen, L. A., Arendt, A. A., Bauder, A., Braithwaite, R. J., Jansson, P., Kaser, G., Möller, M., Nicholson, L., and Zemp, M.: Glossary of glacier mass balance and related terms, IHP-VII Technical Documents in Hydrology No. 86, IACS Contribution No. 2, UNESCOIHP, Paris, France, available at: https://unesdoc.unesco.org/ark:/48223/pf0000192525 (last access: 7 September 2020), 2011.

880   Cruz, R. V., Harasawa, H., Lal, M., Wu, S., Anokhin, Y., Punsalmaa, B., Honda, Y., Jafari, M., Li, C., and Huu Ninh, N.: Asia, in: Climate Change 2007: Impacts, Adaptation and Vulnerability. Contribution of Working Group II to the Fourth Assessment Report of the Intergovernmental Panel on Climate Change, edited by: Parry, M.L., Canziani, O.F., Palutikof, J.P., van der Linden, P.J., and Hanson, C.E., Cambridge University Press, Cambridge, UK, 469–506, https://archive.ipcc.ch/publications_and_data/ar4/wg2/en/ch10.html, 2007.

885   Ding, Y., Sikka, D. R.: Synoptic systems and weather, in: The Asian Monsoon, edited by: Wang, B., Springer, Berlin, Heidelberg, Germany, 131–201, https://doi.org/10.1007/3-540-37722-0_4, 2006.

Dobhal, D. P., Gergan J. T., and Thayyen, R. J.: Mass balance studies of the Dokriani Glacier from 1992 to 2000, Garhwal Himalaya, India, Bull. Glaciol. Res., 25, 9–17, 2008.

Dobhal, D. P., Mehta, M., and Srivastava, D.: Influence of debris cover on terminus retreat and mass changes of Chorabari

890   Glacier, Garhwal region, central Himalaya, India, J. Glaciol., 59, 961–971, https://doi.org/10.3189/2013JoG12J180, 2013.

Elsberg, D.H., Harrison, W. D., Echelmeyer, K. A., and Krimmel, R. M.: Quantifying the effects of climate and surface change on glacier mass balance, J. Glaciol., 47, 649–658, https://doi.org/10.3189/172756501781831783, 2001.

Fujii, Y., Nakawo, M., and Shrestha, M. L.: Mass balance studies of the glaciers in Ridden Valley, Mukut Himal, Seppyo, Special Issue, 38, 17–21, https://doi.org/10.5331/seppyo.38.Special_17, 1976.

895   Fujii, Y., Fujita, K., and Paudyal, P.: Glaciological research in Hidden Valley, Mukut Himal in 1994, Bull. Glaciol. Res., 14, 7–11, 1996.

Fujita, K.: Influence of precipitation seasonality on glacier mass balance and its sensitivity to climate change, Ann. Glaciol., 48, 88–92, https://doi.org/10.3189/172756408784700824, 2008a.

Fujita, K.: Effect of precipitation seasonality on climatic sensitivity of glacier mass balance, Earth Planet. Sci. Lett., 276, 14–

900   19, https://doi.org/10.1016/j.epsl.2008.08.028, 2008b.

Fujita, K. and Nuimura, T.: Spatially heterogeneous wastage of Himalayan glaciers, P. Nat. Acad. Sci. USA, 108, 14011–14014, https://doi.org/10.1073/pnas.1106242108, 2011.

Fujita, K. and Sakai, A.: Modelling runoff from a Himalayan debris-covered glacier, Hydrol. Earth Syst. Sci., 18, 2679–2694, https://doi.org/10.5194/hess-18-2679-2014, 2014.

905 Fujita, K., Nakawo, M., Fujii, Y., and Paudyal, P.: Changes in glaciers in Hidden Valley, Mukut Himal, Nepal Himalayas, from 1974 to 1994, J. Glaciol., 43, 583–588, https://doi.org/10.3189/S002214300000519X, 1997a.

Fujita, K., Sakai, A., and Chhetri, R. B.: Meteorological observation in Langtang Valley, Nepal Himalayas, 1996, Bull. Glaciol. Res., 15, 71–78, 1997b.

Fujita, K., Takeuchi, N., and Seko, K.: Glaciological observations of Yala Glacier in Langtang Valley, Nepal Himalayas, 1994
910 and 1996, Bull. Glaciol. Res., 16, 75–81, 1998.

Fujita, K., Nakazawa, F., and Rana, B.: Glaciological observations on Rikha Samba Glacier in Hidden Valley, Nepal Himalayas, 1998 and 1999, Bull. Glaciol. Res., 18, 31–35, 2001.

Fujita, K., Inoue, H., Izumi, T., Yamaguchi, S., Sadakane, A., Sunako, S., Nishimura, K., Immerzeel, W. W., Shea, J. M., Kayastha, R. B., Sawagaki, T., Breashears, D. F., Yagi, H., and Sakai, A.: Anomalous winter-snow-amplified earthquake-
915 induced disaster of the 2015 Langtang avalanche in Nepal, Nat. Hazards Earth Syst. Sci., 17, 749–764, https://doi.org/10.5194/nhess-17-749-2017, 2017.

Gardelle, J., Berthier, E., and Arnaud, Y.: Impact of resolution and radar penetration on glacier elevation changes computed from DEM differencing, J. Glaciol., 58, 419–422, https://doi.org/10.3189/2012JoG11J175, 2012.

Gardelle, J., Berthier, E., Arnaud, Y., and Kääb, A.: Region-wide glacier mass balances over the Pamir-Karakoram-Himalaya
920 during 1999–2011, The Cryosphere, 7, 1263–1286, https://doi.org/10.5194/tc-7-1263-2013, 2013.

Gardner, A. S., Moholdt, G., Cogley, J. G., Wouters, B., Arendt, A. A., Wahr, J., Berthier, E., Hock, R., Pfeffer, W. T., Kaser, G., Ligtenberg, S. R. M., Bolch, T., Sharp, M. J., Hagen, J.-O. O., van den Broeke, M. R., and Paul, F.: A Reconciled Estimate of Glacier Contributions to Sea Level Rise: 2003 to 2009, Science, 340, 852–857, https://doi.org/10.1126/science.1234532, 2013.

925 GCOS: The Global Observing System for Climate: Implementation Needs, World Meteorological Organization, GCOS-200 (GOOS-214), https://library.wmo.int/doc_num.php?explnum_id=3417, last access: 7 September 2020, 2016.

Gilbert, A., Sinisalo, A., Gurung, T. R., Fujita, K., Maharjan, S. B., Sherpa, T. C., and Fukuda, T.: The influence of water percolation through crevasses on the thermal regime of a Himalayan mountain glacier, The Cryosphere, 14, 1273–1288, https://doi.org/10.5194/tc-14-1273-2020, 2020.

930 Gurung, S., Bhattarai, B. C., Kayastha, R. B., Stumm, D., Joshi, S. P., and Mool, P. K.: Study of annual mass balance (2011–2013) of Rikha Samba Glacier, Hidden Valley, Mustang, Nepal, Sci. Cold Arid Reg., 8, 311–318, https://doi.org/10.3724/SP.J.1226.2016.00311, 2016.

Higuchi, K.: Outline of the Glaciological Expedition of Nepal: Boring Project 1981 and 1982, Bull. Glaciol. Res., 2, 1–13, 1984.

935 Hock, R.: Glacier melt: a review of processes and their modelling, Prog. Phys. Geogr., 29, 362–391. https://doi.org/10.1191/0309133305pp453ra, 2005.

Holzer, N., Vijay, S., Yao, T., Xu, B., Buchroithner, M., and Bolch, T.: Four decades of glacier variations at Muztagh Ata (eastern Pamir): a multi-sensor study including Hexagon KH-9 and Pléiades data, The Cryosphere, 9, 2071–2088, https://doi.org/10.5194/tc-9-2071-2015, 2015.

940 Huss, M.: Density assumptions for converting geodetic glacier volume change to mass change, The Cryosphere, 7, 877–887, https://doi.org/10.5194/tc-7-877-2013, 2013.

Huss, M. and Hock, R.: Global-scale hydrological response to future glacier mass loss. Nat. Clim. Chang., 8, 135-140, https://doi.org/10.1038/s41558-017-0049-x, 2018.

IGOS: Integrated Global Observing Strategy Cryosphere Theme Report - For the Monitoring of our Environment from Space
945 and from Earth, World Meteorological Organization, WMO/TD-No. 1405, 114 pp, https://globalcryospherewatch.org/reference/documents/files/igos_cryosphere_report.pdf, last access: 7 September 2020, 2007.

Iida, H., Watanabe, O., and Takiwaka, M.: First Results from Himalayan Glacier Boring Project in 1981–1982, Part II. Studies on internal structure and transformation process from snow to ice of Yala Glacier, Langtang Himal, Nepal, Bull. Glaciol. Res., 950 2, 25–33, 1984.

Iida, H., Endo, Y., Kohshima, S., Motoyama, H., and Watanabe, O.: Characteristics of snow cover and formation process of dirt layer in the accumulation area of Yala Glacier, Langtang Himal, Nepal, Bull. Glacier Res., 5, 55–62, 1987.

Immerzeel W. W., van Beek, L.P.H., Konz, M., Shrestha, A. B., and Bierkens, M. F. P.: Hydrological response to climate change in a glacierized catchment in the Himalayas, Clim. Change, 110, 721–736, https://doi.org/10.1007/s10584-011-0143-955 4, 2012.

Immerzeel, W. W., Kraaijenbrink, P. D. A., Shea, J. M., Shrestha, A. B., Pellicciotti, F., Bierkens, M. F. P., and de Jong, S.M.: High-resolution monitoring of Himalayan glacier dynamics using unmanned aerial vehicles, Remote. Sens. Environ., 150, 93–103, https://doi.org/10.1016/j.rse.2014.04.025, 2014.

Immerzeel, W. W., Wanders, N., Lutz, A. F., Shea, J. M., and Bierkens, M. F. P.: Reconciling high-altitude precipitation in 960 the upper Indus basin with glacier mass balances and runoff, Hydrol. Earth Syst. Sci., 19, 4673–4687, https://doi.org/10.5194/hess-19-4673-2015, 2015.

Immerzeel, W. W., Lutz, A. F., Andrade, M., Bahl, A., Biemans, H., Bolch, T., Hyde, S., Brumby, S., Davies, B. J., Elmore, A. C., Emmer, A., Feng, M., Fernández, A., Haritashya, U., Kargel, J. S., Koppes, M., Kraaijenbrink, P. D. A., Kulkarni, A. V., Mayewski, P. A., Nepal, S., Pacheco, P., Painter, T. H., Pellicciotti, F., Rajaram, H., Rupper, S., Sinisalo, A., Shrestha, A. 965 B., Viviroli, D., Wada, Y., Xiao, C., Yao, T., and Baillie, J. E. M.: Importance and vulnerability of the world's water towers, Nature, 577, 364–369, https://doi.org/10.1038/s41586-019-1822-y, 2019.

Joerg, P. C., and Zemp, M.: Evaluating volumetric glacier change methods using airborne laser scanning data. Geogr. Ann. Ser. A Phys. Geogr., 96, 135–145, https://doi.org/10.1111/geoa.12036, 2014.

Kääb, A., Berthier, E., Nuth, C., Gardelle, J., and Arnaud, Y.: Contrasting patterns of early twenty-first-century glacier mass 970 change in the Himalayas, Nature, 488, 495–498, https://doi.org/10.1038/nature11324, 2012.

Kargel, J. S., Leonard, G. J., Shugar, D. H., Haritashya, U. K., Bevington, A., Fielding, E. J., Fujita, K., Geertsema, M., Miles, E. S., Steiner, J., Anderson, E., Bajracharya, S., Bawden, G. W., Breashears, D. F., Byers, A., Collins, B., Dhital, M. R., Donnellan, A., Evans, T. L., Geai, M. L,. Glasscoe, M. T., Green, D., Gurung, D. R., Heijenk, R., Hilborn, A., Hudnut, K., Huyck, C., Immerzeel, W. W., Jian, L. M., Jibson, R., Kääb, A., Khanal, N. R., Kirschbaum, D., Kraaijenbrink, P. D. A., 975 Lamsal, D., Liu, S. Y., Lv, M. Y., McKinney, D., Nahirnick, N. K., Nan, Z. T., Ojha, S., Olsenholler, J., Painter, T. H., Pleasants, M., Pratima, K. C., Yuan, Q. I., Raup, B. H., Regmi, D., Rounce, D. R., Sakai, A., Shangguan, D. H., Shea, J. M., Shrestha, A. B., Shukla, A., Stumm, D., van der Kooij, M., Voss, K., Wang, X., Weihs, B., Wolfe, D., Wu, L. Z., Yao, X. J., Yoder, M. R., and Young, N.: Geomorphic and geologic controls of geohazards induced by Nepal's 2015 Gorkha earthquake, Science, 351, aac8353, https://doi.org/10.1126/science.aac8353, 2016.

980 Kappenberger, G., Steinegger, U., Braun, L. N., and Kostka, R., Recent glacier tongues in the Langtang Khola Basin, Nepal, determined by terrestrial photogrammetry, Snow and Glacier Hydrology (Proceedings of the Kathmandu Symposium, November 1992), IAHS Publ. no. 218, 95–101, 1993.

Kaser, G., Grosshauser, M., Marzeion, B.: Contribution potential of glaciers to water availability in different climate regimes. P. Nat. Acad. Sci. USA, 107, 20223-20227, https://doi.org/10.1073/pnas.1008162107, 2010.

985 Kattelmann, R. and Yamada, T.: Storms and Avalanches of November 1995, Khumbu Himal, Nepal. Proceedings of the 1996 International Snow Science Workshop, Banff, Canada, 276–278, 1996.

Koblet, T., Gärtner-Roer, I., Zemp, M., Jansson, P., Thee, P., Haeberli, W., and Holmlund, P.: Reanalysis of multi-temporal aerial images of Storglaciären, Sweden (1959–99) – Part 1: Determination of length, area, and volume changes, The Cryosphere, 4, 333–343, https://doi.org/10.5194/tc-4-333-2010 , 2010.

990 Kostka, R., Schneider, E., Mareich, M., Moser, G., Nairz, W., Patzelt, G., and Schneider, C.: Langthang Himal Ost. In Alpenvereinskarte (Ed.), Alpenvereinskarte, Freytag - Berndt and Artaria, Wien, Austria, 1990.

Lea, J. M., Mair, D. W. F., and Rea, B. R.: Evaluation of existing and new methods of tracking glacier terminus change, J. Glaciol., 60, 323–332. http://doi.org/10.3189/2014JoG13J061, 2014.

Lewis, K. L., Fountain, A. G., and Dana, G. L.: How important is terminus cliff melt?: a study of the Canada Glacier terminus,
995 Taylor Valley, Antarctica, Glob. Planet. Change, 22,105–115, https://doi.org/10.1016/S0921-8181(99)00029-6, 1999.

Lindenmann, J.: Untersuchung dekadischer Gletschervolumenänderungen im Langtang Himalaya, Nepal, basierend auf DHM-Analysen verschiedener Datensätze inklusive statistischer Unsicherheitsanalyse, M.S. thesis, Glaciology and Geomorphodynamics Group - 3G, University of Zurich, Switzerland, 138 pp., 2012.

Litt, M., Shea, J., Wagnon, P., Steiner, J., Koch, I., Stigter, E., and Immerzeel, W.: Glacier ablation and temperature indexed
1000 melt models in the Nepalese Himalaya, Sci. Rep. 9, 5264, https://doi.org/10.1038/s41598-019-41657-5, 2019.

Liu, S., Xie, Z., Song, G., Ma, L., and Ageta, Y.: Glacier on the north side of Mt. Xixiabangma, China, Bull. Glacier Res., 14, 37–43, 1996.

Lutz, A. F., Immerzeel, W. W., Shrestha, A. B., and Bierkens, M.F.P.: Consistent increase in High Asia's runoff due to increasing glacier melt and precipitation, Nature Clim. Change 4, 587–592, https://doi.org/10.1038/nclimate2237, 2014.

1005 Marzeion, B., Jarosch, A. H., and Hofer, M.: Past and future sea-level change from the surface mass balance of glaciers, The Cryosphere, 6, 1295–1322, https://doi.org/10.5194/tc-6-1295-2012, 2012.

Maurer, J. M., Schaefer, J. M., Rupper, S., and Corley, A.: Acceleration of ice loss across the Himalayas over the past 40 years, Sci. Adv. 5, eaav7266, https://doi.org/10.1126/sciadv.aav7266, 2019.

Ménégoz, M., Gallée, H., and Jacobi, H. W.: Precipitation and snow cover in the Himalaya: from reanalysis to regional climate
1010 simulations, Hydrol. Earth Syst. Sci., 17, 3921–3936, https://doi.org/10.5194/hess-17-3921-2013, 2013.

Murakami, S., Ozawa, H., and Yamada, T.: Permeability coefficient of water in snow and firn at the accumulation area of Yala Glacier, Nepal Himalaya, Bull. Glacier Res., 7, 203–208, 1989.

Neckel, N., Kropáček, J., Schröter, B., and Scherer, D.: Effects of Cyclone Hudhud captured by a high altitude Automatic Weather Station in northwestern Nepal, Weather, 70, 208–2010, https://doi.org/10.1002/wea.2494, 2015.

1015 Nuimura, T., Fujita, K., Yamaguchi, S., and Sharma, R. R.: Elevation changes of glaciers revealed by multitemporal digital elevation models calibrated by GPS survey in the Khumbu region, Nepal Himalaya, 1992–2008, J. Glaciol., 58, 648–656, https://doi.org/10.3189/2012JoG11J061, 2012.

Ono, Y.: Recent fluctuations of the Yala (Dakpatsen) Glacier, Langtang Himal, reconstructed from annual moraine ridges, Innsbruck, Z. Gletscher. Glazial., 21, 251–258, 1985.

1020 Ozawa, H.: Thermal regime of a glacier in relation to glacier ice formation, PhD thesis, Sapporo, Hokkaido University, 73 pp., 1991.

Ozawa, H. and Yamada, T: Contributions of internal accumulation to mass balance and conditions of superimposed ice formation in Yala glacier, Nepal Himalayas. In: Report of the Glaciological Expedition of Nepal Himalayas, 1987–1988: Glacial studies in Langtang Valley, Sapporo, Japan, 31–46, 1989.

1025 Paul, F.: Calculation of glacier elevation changes with SRTM: is there an elevation bias? J. Glaciol., 54, 945–946, https://doi.org/10.3189/002214308787779960, 2008.

Pieczonka, T., Bolch, T. Junfeng, W., and Shiyin, L.: Heterogeneous mass loss of glaciers in the Aksu-Tarim Catchment (Central Tien Shan) revealed by 1976 KH-9 Hexagon and 2009 SPOT-5 stereo imagery, Remote. Sens. Environ., 130, 233–244. https://doi.org/10.1016/j.rse.2012.11.020, 2013.

1030 Pratap, B., Dobhal, D. P., Mehta, M., and Bhambri, R.: Influence of debris cover and altitude on glacier surface melting: a case study on Dokriani Glacier, central Himalaya, India, Ann. Glaciol., 56, 9–16, https://doi.org/10.3189/2015AoG70A971, 2015.

Pratap, B., Sharma, P., Patel, L., Singh, A. T., Gaddam, V. K., Oulkar, S., and Thamban, M.: Reconciling High Glacier Surface Melting in Summer with Air Temperature in the Semi-Arid Zone of Western Himalaya, Water, 11, 1561, https://doi.org/10.3390/w11081561, 2019.

1035 Rabus, B., Eineder, M., Roth, A., and Bamler, R.: The shuttle radar topography mission—a new class of digital elevation models acquired by spaceborne radar, ISPRS J. Photogramm. Remote Sens., 57, 241–262, https://doi.org/10.1016/S0924-2716(02)00124-7, 2003.

Racoviteanu, A. E., Armstrong, R., and Williams, M. W.: Evaluation of an ice ablation model to estimate the contribution of melting glacier ice to annual discharge in the Nepal Himalaya, Water Resour. Res., 49, 5117–5133,
1040 https://doi.org/10.1002/wrcr.20370, 2013.

Ragettli, S., Bolch, T., and Pellicciotti, F.: Heterogeneous glacier thinning patterns over the last 40 years in Langtang Himal, Nepal, The Cryosphere, 10, 2075–2097, https://doi.org/10.5194/tc-10-2075-2016, 2016.

Rasmussen, R., Baker, B., Kochendorfer, J., Meyers, T., Landolt, S., Fischer, A. P., Black, J., Thériault, J. M., Kucera, P., Gochis, D., Smith, C., Nitu, R., Hall, M., Ikeda, K., and Gutmann, E.: How Well Are We Measuring Snow: The
1045 NOAA/FAA/NCAR Winter Precipitation Test Bed, B. Am. Meteorol. Soc., 93, 811–829, https://doi.org/10.1175/BAMS-D-11-00052.1, 2012.

Salerno, F., Guyennon, N., Thakuri, S., Viviano, G., Romano, E., Vuillermoz, E., Cristofanelli, P., Stocchi, P., Agrillo, G., Ma, Y., and Tartari, G.: Weak precipitation, warm winters and springs impact glaciers of south slopes of Mt. Everest (central Himalaya) in the last 2 decades (1994–2013), The Cryosphere, 9, 1229–1247, https://doi.org/10.5194/tc-9-1229-2015, 2015.

1050 Sakai, A., Nakawo, M. and Fujita, K.: distribution characteristics and energy balance of ice cliffs on debris-covered Glaciers, Nepal Himalaya, Arct. Antarct. Alp. Res., 34, 12–19, https://doi.org/10.1080/15230430.2002.12003463, 2002.

Schwitter, M. P. and Raymond, C. F.: Changes in the longitudinal profiles of glaciers during advance and retreat, J. Glaciol., 39, 582–590, https://doi.org/10.3189/S0022143000016476, 1993.

Seko, K. and Takahashi, S.: Characteristics of Winter Precipitation and its Effect on Glaciers in the Nepal Himalaya, Bull.
1055 Glaciol. Res., 9, 9–16, 1991.

Shea, J. M., Immerzeel, W. W., Wagnon, P., Vincent, C., and Bajracharya, S.: Modelling glacier change in the Everest region, Nepal Himalaya, The Cryosphere, 9, 1105–1128, https://doi.org/10.5194/tc-9-1105-2015, 2015a.

Shea, J. M., Wagnon, P., Immerzeel, W. W., Biron, R., Brun, F., and Pellicciotti, F.: A comparative high-altitude meteorological analysis from three catchments in the Nepalese Himalaya, Int. J. Water Res. Environ. Eng.,
1060 https://doi.org/10.1080/07900627.2015.1020417, 2015b.

Sherpa, S. F., Wagnon, P., Brun, F., Berthier, E., Vincent, C., Lejeune, Y., Arnaud, Y., Kayastha, R.B., and Sinisalo, A.: Contrasted surface mass balances of debris-free glaciers observed between the southern and the inner parts of the Everest region (2007–15), J. Glaciol., 63, 637–651, https://doi.org/10.1017/jog.2017.30, 2017.

Shrestha, M.L., Fujii, Y., and Nakawo, M.: Climate of Hidden Valley, Mukut Himal during the Monsoon in 1974, Seppyo, 38
1065 105–108, https://doi.org/10.5331/seppyo.38.Special_105, 1976.

Shiraiwa, T.: Glacial fluctuations and cryogenic environments in the Langtang Valley, Nepal Himalaya, PhD thesis, Hokkaido University, Sapporo, Japan, 230 pp., http://doi.org/10.11501/3071619, 1993.

Shiraiwa, T.: Glacial fluctuations and cryogenic environments in the Langtang Valley, Nepal Himalaya, Contribution from the Institute of Low Temperature Science, Series A, 38, 1-98, http://hdl.handle.net/2115/20256, last access: 7August 2020, 1994.

1070 Shiraiwa, T. and Watanabe, T.: Late Quaternary Glacial Fluctuations in the Langtang Valley, Nepal Himalaya, Reconstructed by Relative Dating Methods, Arct. Antarct. Alp. Res., 23, 404–416, https://doi.org/10.1080/00040851.1991.12002860, 1991.

Shiraiwa, T., Kenichi, U., and Yamada, T.: Distribution of mass input on glaciers in the Langtang Valley, Nepal Himalayas, Bull. Glacier Res., 10, 21–30, 1992.

Sommer, C., Malz, P., Seehaus, T.C., Lippl, S., Zemp, M. and Braun, M. H.: Rapid glacier retreat and downwasting throughout

1075    the European Alps in the early 21st century. Nat. Commun., 11, 3209, https://doi.org/10.1038/s41467-020-16818-0, 2020.

Steinegger, U., Braun, L. N., Kappenberger, G., and Tartari, G.: Assessment of Annual Snow Accumulation over the Past 10 Years at High Elevations in the Langtang Region, Snow and Glacier Hydrology (Proceedings of the Kathmandu Symposium, November 1992), IAHS Publ. no. 218, 155–166, 1993.

Steiner, J. F., Pellicciotti, F., Buri, P., and Miles, E. S.: Modelling ice-cliff backwasting on a debris- covered glacier in the

1080    Nepalese Himalaya, J. Glaciol., 61, 889¬–907, https://doi.org/10.3189/2015JoG14J194, 2015.

Stigter, E. E., Litt, M., Steiner, J. F., Bonekamp, P. N. J., Shea, J. M., Bierkens, M. F. P., and Immerzeel, W. W.: The Importance of Snow Sublimation on a Himalayan Glacier, Front. Earth Sci., 6, https://doi.org/10.3389/feart.2018.00108, 2018.

Sugiyama, S., Kukui, K., Fujita, K., Tone, K., and Yamaguchi, S.: Changes in ice thickness and flow velocity of Yala Glacier, Langtang Himal, Nepal, from 1982 to 2009, Ann. Glaciol., 54, 157–162, https://doi.org/10.3189/2013AoG64A111, 2013.

1085    Takagi, H., Kazunori, A., Danhara, T., and Hideki, I.: Timing of the Tsergo Ri landslide, Langtang Himal, determined by fission-track dating of pseudotachylyte, J. Asian Earth Sci., 29, 466–472, https://doi.org/10.1016/j.jseaes.2005.12.002, 2007

Takahashi, S., Motoyama, H., Kawashima, K, Morinaga, Y., Seko, K, Iida, H., Kubota, H., and Turadahr, N. R.: Meteorological features in Langtang Valley, Nepal Himalayas, 1985–1986, Bull. Glaciol. Res., 5, 35–40, 1987a.

Takahashi, S., Motoyama, H., Kawashima, K, Morinaga, Y., Seko, K, Iida, H., Kubota, H., and Turadahr, N. R.: Summery of

1090    meteorological data at Kyangchen in Langtang Valley, Nepal Himalayas, Bull. Glaciol. Res., 5, 121–128, 1987b.

Tawde, S. A., Kulkarni, A.V., and Bala, G.: An estimate of glacier mass balance for the Chandra basin, western Himalaya, for the period 1984–2012, Ann. Glaciol., 58, 99–109, https://doi.org/10.1017/aog.2017.18, 2017.

Tian, L., Zong, J., Yao, T., Ma,L., Pu, J., and Zhu, D.: Direct measurement of glacier thinning on the southern Tibetan Plateau (Gurenhekou, Kangwure and Naimona'Nyi glaciers), J. Glaciol., 60, 879–888, https://doi.org/10.3189/2014JoG14J022, 2014.

1095    Tshering, P. and Fujita, K.: First in situ record of decadal glacier mass balance (2003–2014) from the Bhutan Himalaya, Ann. Glaciol., 57, 289–294, https://doi.org/10.3189/2016AoG71A036, 2016.

Vincent, C., Ramanathan, Al., Wagnon, P., Dobhal, D. P., Linda, A., Berthier, E., Sharma, P., Arnaud, Y., Azam, M. F., Jose, P. G., and Gardelle, J.: Balanced conditions or slight mass gain of glaciers in the Lahaul and Spiti region (northern India, Himalaya) during the nineties preceded recent mass loss, The Cryosphere, 7, 569–582, https://doi.org/10.5194/tc-7-569-2013,

1100    2013.

Wagnon, P., Linda, A., Arnaud, Y., Kumar, R., Sharma, P., Vincent, C., Pottakkal, J. G., Berthier, E., Ramanathan, A., Hasnain, S.I., and Chevallier, P.: Four years of mass balance on Chhota Shigri Glacier, Himachal Pradesh, India, a new benchmark glacier in the western Himalaya, J. Glaciol., 53, 603–611, https://doi.org/10.3189/002214307784409306, 2007.

Wagnon, P., Vincent, C., Arnaud, Y., Berthier, E., Vuillermoz, E., Gruber, S., Ménégoz, M., Gilbert, A., Dumont, M., Shea,

1105    J. M., Stumm, D., and Pokhrel, B. K.: Seasonal and annual mass balances of Mera and Pokalde glaciers (Nepal Himalaya) since 2007, The Cryosphere, 7, 1769–1786, https://doi.org/10.5194/tc-7-1769-2013, 2013.

Wagnon, P., Brun, F., Khadka, A., Berthier, E., Shrestha, D., Vincent, C., Arnaud, Y., Six, D., Dehecq, A., Ménégoz, M., and Jomelli, V.: Reanalysing the 2007–19 glaciological mass-balance series of Mera Glacier, Nepal, Central Himalaya, using geodetic mass balance, J. Glaciol., 1–9, https://doi.org/10.1017/jog.2020.88, 2020.

1110    Watanabe, O., Takenaka, S., Iida, H., Kamiyama, K., Thapa, K. B., and Mulmi, D. D.: First results from Himalayan glacier boring project in 1981–1982, Part I. Stratigraphic analyses of full-depth cores from Yala Glacier, Langtang Himal, Nepal, Bull. Glacier Res., 2, 7–23, 1984.

Weidinger, J. T., Schramm, J. M., and Nuschej, F.: Ore mineralization causing slope failure in a high-altitude mountain crest—on the collapse of an 8000 m peak in Nepal, J. Asian Earth Sci., 21, 295–306, https://doi.org/10.1016/S1367-9120(02)00080-

1115    9, 2002.

Winkler, M., Kaser, G., Cullen, N., Mölg, T., Hardy, D., & Pfeffer, W.: Land-based marginal ice cliffs: Focus on Kilimanjaro, Erdkunde, 64, 179–193. https://doi.org/10.3112/erdkunde.2010.02.05, 2010.

WGMS: Global Glacier Change Bulletin No. 1 (2012–2013), edited by: Zemp, M., Gärtner-Roer, I., Nussbaumer, S. U., Hüsler, F., Machguth, H., Mölg, N., Paul, F., and Hoelzle, M.: ICSU(WDS)/IUGG(IACS)/ UNEP/UNESCO/WMO, World

1120    Glacier Monitoring Service, Zurich, Switzerland, Publication based on database version: doi:10.5904/wgms-fog-2015-11, Zurich, Switzerland, available at: http://wgms.ch/ggcb/ (last access: 7 September 2020), 2015.

WGMS: Global Glacier Change Bulletin No. 2 (2014–2015), edited by: Zemp, M., Nussbaumer, S. U., Gärtner-Roer, I., Huber, J., Machguth, H., Paul, F., and Hoelzle, M.: ICSU(WDS)/IUGG(IACS)/UNEP/UNESCO/WMO, World Glacier Monitoring Service. Publication based on database version: https://doi.org/10.5904/wgms-fog-2017-10, Zurich, Switzerland, available at:

1125    http://wgms.ch/ggcb/ (last access: 7 September 2020), 2017.

WGMS: Fluctuations of Glaciers Database, World Glacier Monitoring Service, digital media, http://dx.doi.org/10.5904/wgms-fog-2020-08, 2020a.

WGMS: Global Glacier Change Bulletin No. 3 (2016–2017), edited by: Zemp, M., Gärtner-Roer, I., Nussbaumer, S.U., Bannwart, J., Rastner, P., Paul, F., and Hoelzle, M., ISC(WDS)/IUGG(IACS)/UNEP/UNESCO/WMO, World Glacier

1130    Monitoring Service, Zurich, Switzerland, available at: http://wgms.ch/downloads/WGMS_GGCB_03.pdf, last access: 7 September 2020, 2020b.

Yamada, T., Motoyama, H., and Thapa, K.B.: Mass balance study of a glacier system from hydrological observations in Langtang Valley, Nepal Himalaya, Ann. Glaciol., 6, 318–320, https://doi.org/10.3189/1985AoG6-1-318-320, 1985.

Yamada, T., Shiraiwa, T., Iida, H., Kadota, T., Watanabe, T., Rana, B., Ageta, Y., and Fushimi, H.: Fluctuations of the glaciers

1135    from the 1970s to 1989 in the Khumbu, Shorong and Langtang regions, Nepal Himalayas, Bull. Glaciol. Res., 10, 11–19, 1992.

Yokoyama, K.: Ground Photogrammetry of Yala Glacier, Langtang Himal, Nepal Himalaya, Bull. Glaciol. Res., 2, 99–105, 1984.

Yoshimura, Y., Kohshima, S., Takeuchi, N., Seko, K., and Fujita, K.: Snow algae in a Himalayan ice core: new environmental markers for ice-core analyses and their correlation with summer mass balance, Ann. Glaciol., 43, 148–153,

1140    https://doi.org/10.3189/172756406781812276, 2006.

Zemp, M., Thibert, E., Huss, M., Stumm, D., Rolstad Denby, C., Nuth, C., Nussbaumer, S. U., Moholdt, G., Mercer, A., Mayer, C., Joerg, P. C., Jansson, P., Hynek, B., Fischer, A., Escher-Vetter, H., Elvehøy, H., and Andreassen, L. M.: Reanalysing glacier mass balance measurement series, The Cryosphere, 7, 1227–1245, https://doi.org/10.5194/tc-7-1227-2013, 2013.

1145    Zemp, M., Huss, M., Eckert, N., Thibert, E., Paul, F., Nussbaumer, S. U., and Gärtner-Roer, I.: Brief communication: Ad hoc estimation of glacier contributions to sea-level rise from the latest glaciological observations, The Cryosphere, 14, 1043–1050, https://doi.org/10.5194/tc-14-1043–2020, 2020.